MARTIN MARIETTA ENERGY SYSTEMS LIBRARIES
3 4456 0361392 6

CENTRAL RESEARCH LIBRARY
DOCUMENT COLLECTION

ORNL-2740
Physics and Mathematics
TID-4500 (14th ed.)

ELECTRONUCLEAR RESEARCH DIVISION

ANNUAL PROGRESS REPORT

FOR PERIOD ENDING OCTOBER 1, 1958

CENTRAL RESEARCH LIBRARY
DOCUMENT COLLECTION
LIBRARY LOAN COPY
DO NOT TRANSFER TO ANOTHER PERSON
If you wish someone else to see this document, send in name with document and the library will arrange a loan.

OAK RIDGE NATIONAL LABORATORY
operated by
UNION CARBIDE CORPORATION
for the
U.S. ATOMIC ENERGY COMMISSION

Printed in USA. Price $1.50. Available from the

Office of Technical Services
Department of Commerce
Washington 25, D.C.

LEGAL NOTICE

This report was prepared as an account of Government sponsored work. Neither the United States, nor the Commission, nor any person acting on behalf of the Commission:

A. Makes any warranty or representation, expressed or implied, with respect to the accuracy, completeness, or usefulness of the information contained in this report, or that the use of any information, apparatus, method, or process disclosed in this report may not infringe privately owned rights; or

B. Assumes any liabilities with respect to the use of, or for damages resulting from the use of any information, apparatus, method, or process disclosed in this report.

As used in the above, "person acting on behalf of the Commission" includes any employee or contractor of the Commission, or employee of such contractor, to the extent that such employee or contractor of the Commission, or employee of such contractor prepares, disseminates, or provides access to, any information pursuant to his employment or contract with the Commission, or his employment with such contractor.

ORNL-2740
Physics and Mathematics
TID-4500 (14th ed.)

Contract No. W-7405-eng-26

ELECTRONUCLEAR RESEARCH DIVISION

ANNUAL PROGRESS REPORT

For Period Ending October 1, 1958

Robert S. Livingston, Director

DATE ISSUED

JUN 2 1959

OAK RIDGE NATIONAL LABORATORY
Oak Ridge, Tennessee
operated by
UNION CARBIDE CORPORATION
for the
U.S. ATOMIC ENERGY COMMISSION

MARTIN MARIETTA ENERGY SYSTEMS LIBRARIES

3 4456 0361392 6

CONTENTS

ABSTRACT..... 1
HEAVY-PARTICLE PHYSICS..... 1
Evaporation Reactions..... 2
Elastic Scattering of N^{14} by Be^{9}..... 6
THE 86-in. CYCLOTRON..... 9
Nuclear Physics Research..... 10
Applied Physics..... 15
ELECTRONUCLEAR MACHINES..... 18
Cyclotron Analogue I..... 19
Cyclotron Analogue II..... 25
THE OAK RIDGE RELATIVISTIC ISOCHRONOUS CYCLOTRON..... 33
PUBLICATIONS..... 41
ANNOUNCEMENTS..... 45

ELECTRONUCLEAR RESEARCH DIVISION ANNUAL PROGRESS REPORT

ABSTRACT

A wide range of nitrogen-induced nuclear reactions was investigated with the ORNL 63-Inch Cyclotron. Reactions in which only one particle is emitted are found to be more probable than would be expected. The angular distributions of the light particles emitted are being investigated, and studies are being made of the scattering of incident nitrogen ions.

The 23-Mev protons from the ORNL 86-Inch Cyclotron are being used in investigations of the details of proton scattering from various elements, of proton-induced fission, and of nuclear levels excited in nuclei of the rare earths.

The successful operation and predictable performance of the 200-kev electron cyclotron have served to validate extensive theoretical studies of ion orbits and the optical properties of azimuthally varying magnetic fields (AVF). A second cyclotron analogue is being designed to accelerate electrons to ~500 kev in an eight-sector spiral AVF magnet.

A feasibility study was completed for the construction of a variable-energy, three-sector, azimuthally-varying-field, 76-in., fixed-frequency cyclotron designed to accelerate various particles with e/m ratios from 1 to 0.125 over a wide range of energies, including protons to 75 Mev. The new machine is to be known as the Oak Ridge Relativistic Isochronous Cyclotron (ORIC).

HEAVY-PARTICLE PHYSICS

The heavy-ion physics program based on 28-Mev N^{+++} ions accelerated in the ORNL 63-Inch Cyclotron has been concentrated along two main lines of research: the investigation of nuclear reactions in which light particles are emitted and the study of elastic scattering. In addition, considerable effort was devoted to a measurement of the density of a high-voltage carbon arc, of interest in the work on controlled thermonuclear reactions.

Evaporation Reactions

The largest part of the cross section for heavy-ion nuclear reactions on the lighter nuclei is characterized by the emission of light fragments, protons, neutrons, deuterons, tritons, or alpha particles, while the rest of the nuclear matter remains in the form of a residual nucleus. This type of reaction has, in the past year, been investigated in many ways. Absolute cross sections were measured for reactions which lead to radioactive residual nuclei; energy spectra of light particles were determined, as well as, in some cases, their angular distributions and the relative probabilities for the emission of protons, deuterons, and alpha particles. There is at present no theory which describes these nuclear reactions. The approach has been to assume that the reactions proceed by formation of a highly excited compound nucleus followed by its subsequent de-excitation through a statistical emission of light particles. In this way it may be ascertained whether such a mechanism adequately describes the results obtained; whether there are any systematic trends in these reactions, depending, say, on the atomic number of the nucleus or its even-odd character; whether there are any sharp deviations from smooth trends; and what the most sensitive parameters in the interpretation of the data are.

Total-Cross-Section Measurements. — During the past year the excitation functions were measured for the following reactions:

1. $S^{32}(N^{14},p)Ti^{45}$
2. $S^{32}(N^{14},2p)Sc^{44}$
3. $S^{32}(N^{14},2p)Sc^{44\underline{m}}$
4. $S^{32}(N^{14},2pn)Sc^{43}$
5. $S^{32}(N^{14},2\alpha)K^{38\underline{m}}$
6. $K^{39}(N^{14},n)Fe^{52}$
7. $K^{39}(N^{14},p)Mn^{52\underline{m}}$
8. $K^{39}(N^{14},p)Mn^{52}$
9. $K^{39}(N^{14},pn)Mn^{51}$
10. $K^{39}(N^{14},\alpha)Cr^{49}$
11. $K^{39}(N^{14},\alpha p)V^{48}$
12. $K^{39}(N^{14},\alpha pn)V^{47}$
13. $K^{39}(N^{14},2\alpha)Ti^{45}$

Cross sections of reactions 1, 2 and 3, and 5 were compared with calculations based on a statistical evaporation of particles from the compound nucleus. Two values of a in the level density formula $w = C \exp 2(aE^*)^{1/2}$

were used: a = A/10.5 as suggested by Lang and LeCouteur, and a lower value, a = 2, which seems to fit a great deal of this type of data obtained from reactions induced by neutrons or alpha particles. Since the absolute values of the cross sections depend on the formation cross section, which cannot be reliably calculated, ratios of experimental cross sections are compared with calculated ratios. Table 1 shows these ratios for the two values of a, each one with and without gamma de-excitation in competition with particle de-excitation. Details of the measurements and

Table 1. Comparison of Calculated and Experimental Cross Sections at 27 Mev

Ratio of Cross Sections	Experimental Values	Calculated Values			
		Gamma Emission Included		Gamma Emission Excluded	
		a = A/10.5	a = 2	a = A/10.5	a = 2
$\frac{Ti^{45}, p}{Sc^{44}, 2p}$	0.024	0.025	0.16	0.0047	0.032
$\frac{Ti^{45}, p}{K^{38m}, 2\alpha}$	1.1	4.7	3.0	0.50	0.47

the calculations will be published elsewhere.[1] It may be seen from the table that a = A/10.5 with gamma competition and a = 2 without gamma competition fit the data as well as can be expected. The question of the importance of gamma de-excitation is still open; however, the results indicate that it cannot be summarily dismissed, as has been done by many workers heretofore.

Table 2 lists the nuclear reactions from the nitrogen bombardment of potassium and the measured cross sections. By making certain assumptions about the total cross section, it may be deduced from the results listed in the table that reactions in which only one particle is emitted are more

[1]D. E. Fisher, A. Zucker, and A. Groff, Nuclear Reactions Induced by the Nitrogen Bombardment of Sulfur, submitted to Phys. Rev.

Table 2. Cross Sections for Production of Radioactive Nuclides by N^{14} Bombardment of Potassium

Assumed Target Nucleus	Observed Residual Nucleus	Assumed De-excitation Mode	Cross Section (mb) At				
			23.5 Mev	24.5 Mev	25.5 Mev	26.5 Mev	27.5 Mev
K^{39}	Fe^{52}	n		0.012	0.033	0.074	0.14
K^{39}	Mn^{52}	p		0.23	0.62	1.5	3.1
K^{39}	Mn^{52m}	p			0.35	0.66	0.95
K^{39}	Cr^{49}	α			0.055	0.14	0.32
K^{39}	Mn^{51}	pn + 2n	0.26	0.82	2.1	4.6	8.3
K^{39}	V^{48}	αp			1.4	3.4	6.7
K^{39}	V^{47}	pn + 2n		0.088	0.25	0.44	0.57
K^{39}	Ti^{45}	2α		0.070	0.28	0.62	1.6
K^{41}	Fe^{53}	2n		0.19	0.51	1.3	2.9

probable than would be expected from measured particle spectra from the nitrogen-aluminum reactions. This excess of single-particle emission has been noted before, and its significance merits further examination. Again the reader is referred to the published work[2] for details concerning this work.

Light-Particle Distributions. — Energy spectra have now been measured for light particles from Li^6, Li^7, Be^9, C^{12}, N^{14}, O^{16}, and Al^{27}. In the last two cases angular distributions in the forward hemisphere were also measured. The spectra of all these particles may be represented fairly closely by straight lines if they are corrected for barrier penetration and phase space and plotted as a function of the square root of the excitation energy, E^*, in the residual nucleus. In terms of an approximate Fermi gas model a plot of this type allows one to determine directly the

[2]J. J. Pinajian and M. L. Halbert, Nitrogen-Induced Nuclear Reactions in Potassium, submitted to Phys. Rev.

constant a in the level density formula $w = C \exp 2(aE^*)^{1/2}$. In two instances the data could be fitted only if an additional constant b was subtracted from E^* in the level density formula. The values of a and b are listed in Table 3 for all the reactions studied. An increase in a as a function of atomic number may be seen. Only a general trend may be discerned, and all the points do not by any means lie on a smooth curve.

The relative probability for the emission of various particles was also determined for the nitrogen-induced reactions in the elements listed. Without going into detail it can be stated that the probability of emission in most cases does not depend on the type of particle but rather only on the characteristics of the residual nucleus. Stated another way, this

Table 3. Values of a and b for All Reactions Studied

Target	Residual Nucleus	Particle	a	b
Li^6	F^{19}	p	1.1	0
	O^{16}	α		
Li^7	F^{20}	p	1.4	0
	F^{19}	d	1.1	0
	O^{17}	α		
Be^9	Ne^{22}	p	2.6	4.9
	Ne^{21}	d	1.4	0
	Ne^{20}	t	2.6	4.9
	F^{19}	α	1.1	0
N^{14}	Al^{27}	p		
	Al^{26}	d	2.2	
O^{16}	Si^{29}	p	2.5	0
	Si^{28}	d		
	Al^{26}	α	1.3	0
Al^{27}	K^{40}	p	5.0	0
	A^{37}	α	4.1	0

means that the statistical emission of complex fragments such as alpha particles or deuterons is as probable as the emission of protons. For the purpose of these comparisons such factors as phase space, barrier, and spin have been eliminated.

So far, four angular distributions have been measured, protons and alpha particles from aluminum and oxygen targets. In both cases the protons were found to be fairly isotropic, as were alpha particles from aluminum. However, alpha particles from oxygen targets were found to be emitted preferentially in the forward direction. This angular distribution is shown in Fig. 1.

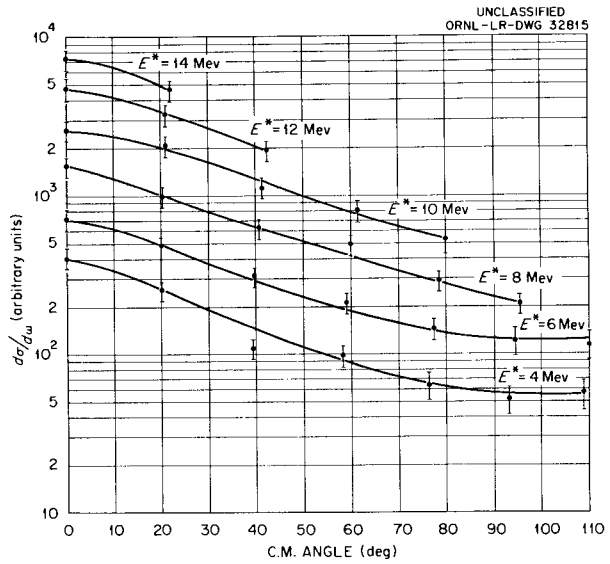

Fig. 1. Angular Distribution of Alpha Particles from the Nitrogen Bombardment of Oxygen. The relative cross sections at various excitation energies are correctly represented by the ordinate.

Elastic Scattering of N^{14} by Be^9

Thin foils of Be^9 (0.2 mg/cm^2) are being bombarded with 27.9-Mev N^{14} ions in the 24-in.-dia scattering chamber. The scattered N^{14} ions are detected with a CsI(Tl) scintillation detector. The angle it makes with the incident beam direction can be set from outside the chamber to an accuracy of ±0.1°. The counter accepts particles emitted from the target in a cone of half angle 0.2 or 0.4°, depending on the choice of collimator.

The energy resolution of this detector is insufficient for a clear distinction to be made between the elastic and inelastic scattering from the Be^9, or between the N^{14} scattered by the Be^9 and that scattered by impurities such as carbon and oxygen. To eliminate the unwanted counts, a second, independently movable scintillation counter is used to detect the recoil particle in coincidence with the N^{14}. For any setting of the N^{14} counter, the angle at which the recoil particle is detected is unique for a given scattering process, and it is easy to distinguish Be^9 elastic

scattering from other events. The coincidence method is similarly well adapted for rejection of pulses from nuclear reactions in the Be^9 or in the impurities.

Figure 2 shows typical spectra of N^{14} scattered at 20°. The upper spectrum was ungated, while the lower one was gated by coincidences with the second counter at the proper angle for detection of the recoil Be^9 ions. Figure 3 shows coincidence-gated spectra with the second counter set at various angles. The peak in the 70.3° spectrum is probably due to N^{14} scattered from oxygen impurity atoms. The area of the main peak remains the same for several degrees on either side of 64.3°, indicating that the aperture of the second counter is large enough to accept all recoil Be^9 ions in coincidence with the N^{14} detected by the first counter.

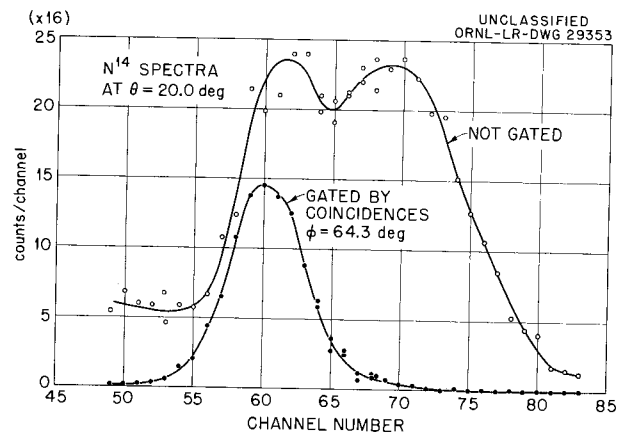

Fig. 2. Pulse-Height Distributions of Counts in the Defining Counter Gated and Ungated by a Second Counter in Coincidence. ϕ = 64.3° is the laboratory angle at which Be recoils are expected for elastically scattered nitrogen detected at 20° in the laboratory system.

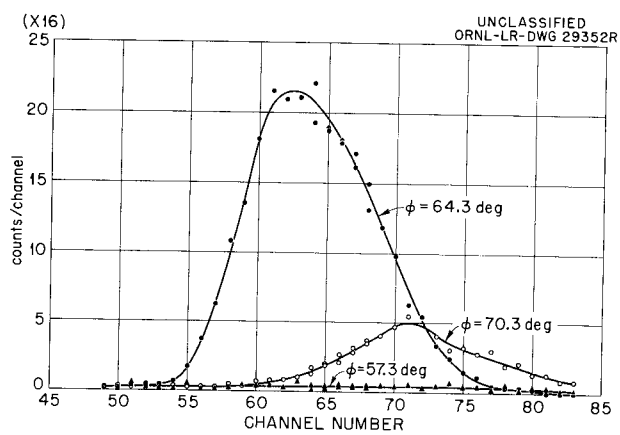

Fig. 3. Pulse-Height Distributions in the Defining Counter Gated by the Conjugate Counter at Various Angles, ϕ, in the Laboratory System.

The counting rate relative to that at 25° was measured at 1.25° intervals from 12.5 to 32.5°. These laboratory angles correspond approximately to the center-of-mass angles 33 to 90°. At all angles the coincidence rate as a function of the position of the second counter was checked to ensure that the first counter was defining the solid angle for detection of coincidences. Runs at many angles were made several days or weeks apart; the data were usually reproduced within the accuracy expected.

Experimental difficulties are encountered at the smallest and the largest angles studied. At small N^{14} angles the recoil Be^9 is emitted at large angles with very low energy. Its energy loss in the target is minimized by tilting the target so that the Be^9 does not pass through it at a steep angle. Careful checks of coincidence rate vs threshold setting for the Be^9 counter have been made to show that all these low-energy Be^9 ions are being detected. At the smallest angle a series of runs was made in which the diameter of the collimator in front of the Be^9 counter was progressively reduced. The results indicated that multiple scattering of the Be^9 ions as they left the target would not cause loss of coincidences at 12.5° or larger N^{14} angles, but would probably create a serious problem at smaller angles. There does not appear to be any satisfactory way of extending the measurements to smaller angles with the present apparatus and targets.

At the largest angles multiple scattering of the N^{14} coupled with the low counting rate make reliable measurements difficult. Fortunately, by simply reversing the roles of the counters, it is possible to extend the measurements to much larger angles. That is, the Be^9 is detected by the small-aperture counter, while the large-aperture second counter serves to gate the pulse-height analyzer with coincident N^{14} pulses. Thus, multiple scattering of the N^{14} no longer constitutes a problem, except possibly at very large scattering angles where the N^{14} energy is very low.

Actually, this reversal of counters is practically essential for another reason. Because the incident projectiles are heavier than the target particles, near the 40° laboratory angle a large center-of-mass solid-angle interval for the N^{14} is compressed into a small laboratory interval. No such compression occurs for the Be^9.

This series of runs is not yet completed. Thus far measurements of counting rates relative to that at 85° have been made out to 132° (center-of-mass angles).

Figure 4 shows the experimental results (converted to the center-of-mass system) which were obtained with the N^{14} detected by the small-aperture counter. The new data with the Be^{9} counter defining the solid angle is not included. It continues the downward trend, but some structure is evident. The Coulomb curve shown is the expected counting rate calculated from the target thickness and integrated beam. The ordinate is reliable to no better than about 20% because of uncertainty in the target thickness.

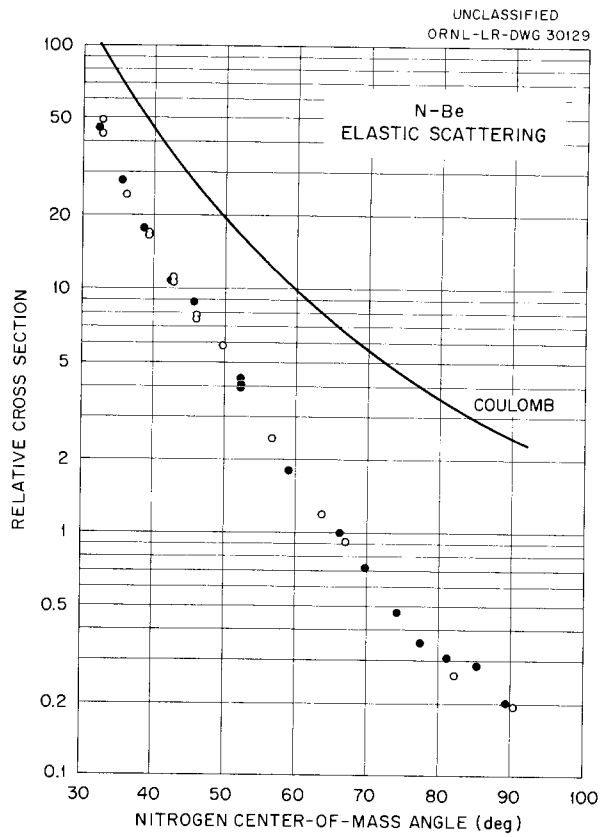

Fig. 4. Differential Cross Section of N^{14}-Be^{9} Elastic Scattering as a Function of the Nitrogen C-M Angle. The upper curve is the cross section for Coulomb scattering.

THE 86-in. CYCLOTRON

Operation of the 86-in. cyclotron continued throughout the year without major interruption. The machine is now operating on an 80-hr-week schedule. Actual "on-beam" time averaged about 50%. The deflected beam available for nuclear physics work at the remote target 40 ft from the cyclotron exceeds requirements; a beam of ~80 μa of ~25-Mev protons can be used on a target at an intermediate position. For applied physics work, a steady circulating beam of over 2 ma is available on large internal targets. Change-over is readily made between internal and external targets.

Nuclear Physics Research

Direct interaction inelastic scattering (DIIS) of 23-Mev protons by medium and heavy elements was studied[1] with magnetic analysis of sufficiently good resolution to separate reactions leading to individual levels. These results are shown in Figs. 5, 6, and 7. A comparison with available data from Coulomb excitation shows a level-to-level correlation between B(E2) and the cross section for DIIS; that is, those levels which are strongly excited by Coulomb excitation also have large DIIS cross sections. A reverse correlation exists between DIIS and (p,d) and (d,p) reactions (Fig. 8). This indicates that DIIS preferentially excites collective levels. As a result of these studies and other evidence, "anomalous inelastic scattering"[2] is now believed to be due to some type of collective excitation "dissolved" among many shell model states in that energy region.

The energy distributions of protons, deuterons, tritons, and alpha

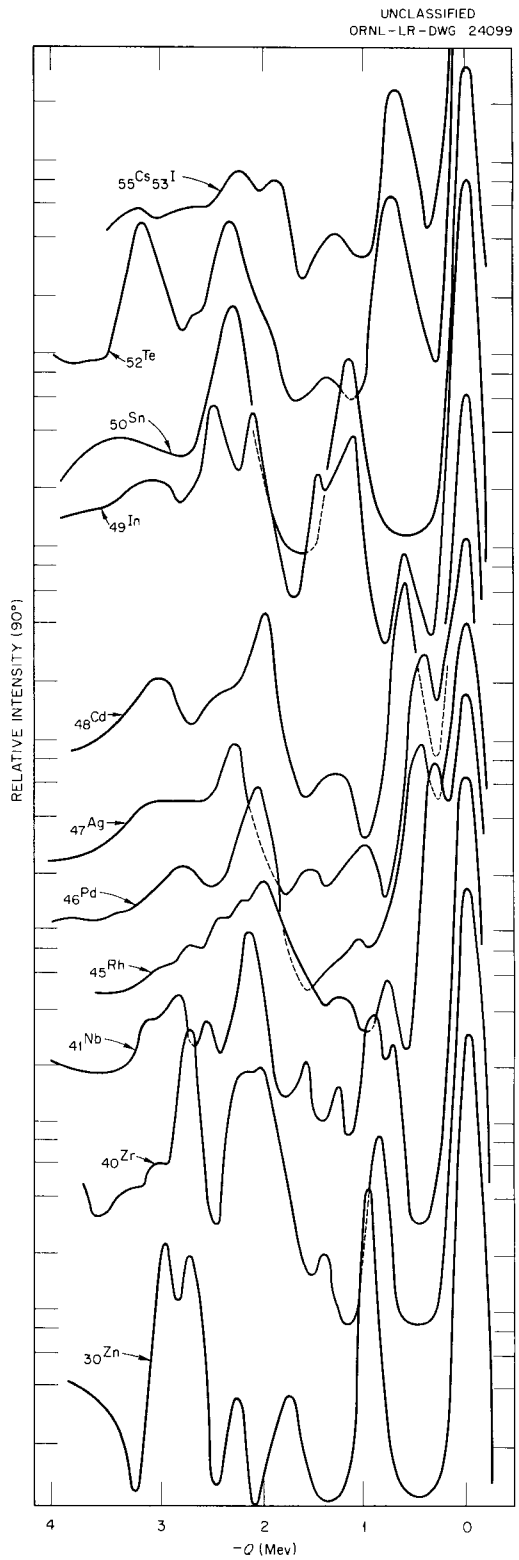

Fig. 5. Energy Distribution of Protons Inelastically Scattered from Various Elements (Atomic Numbers 40–55 and Zinc) as Measured with Magnetic Analysis. Observation angle was 90°.

[1]B. L. Cohen and A. G. Rubin, Phys. Rev. 111, 1568 (1958).

[2]B. L. Cohen, Phys. Rev. 105, 1549 (1957).

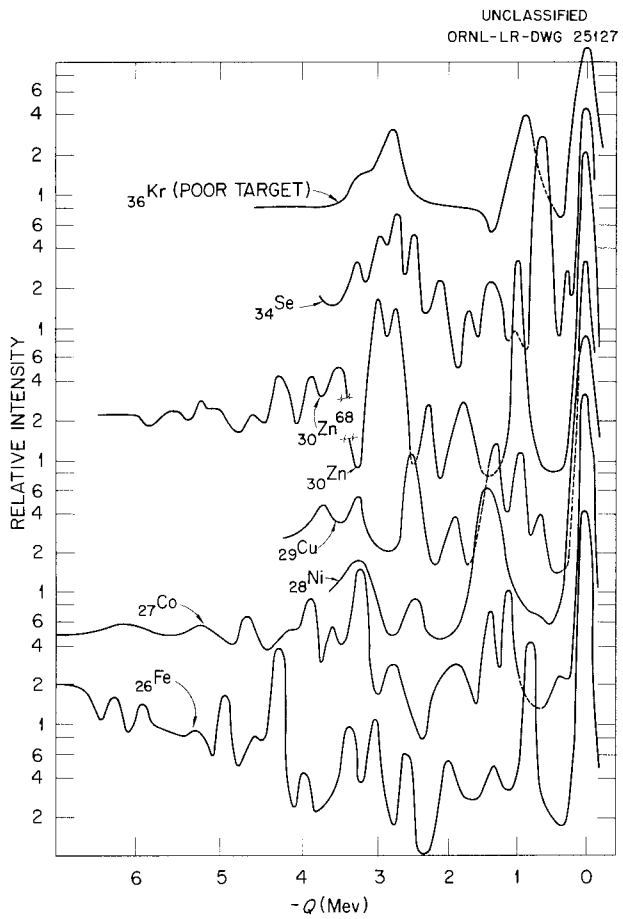

Fig. 6. Energy Distribution of Protons Inelastically Scattered from Various Elements (Atomic Numbers 26–36) as Measured with Magnetic Analysis. Observation angle was 90°.

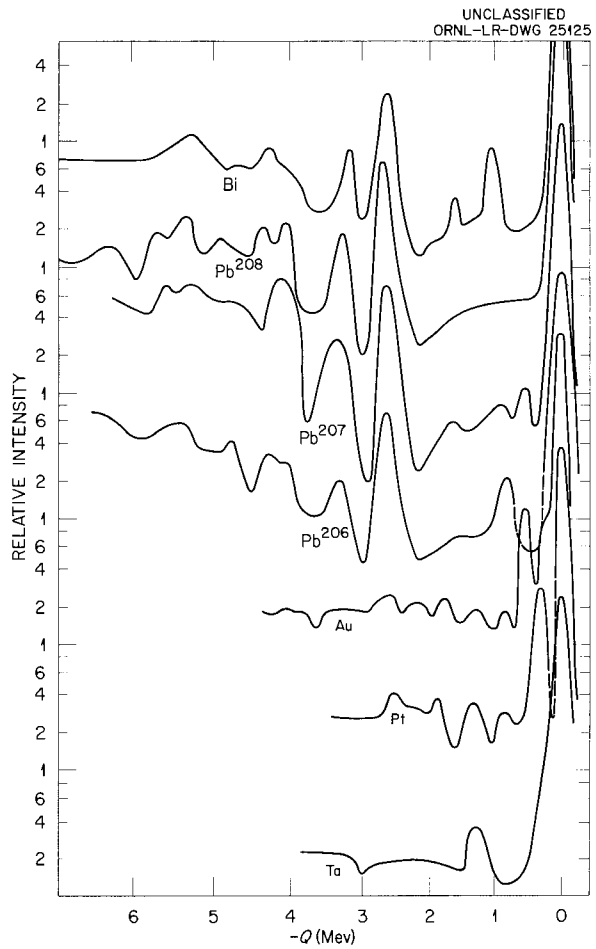

Fig. 7. Energy Distribution of Protons Inelastically Scattered from Various Elements (Atomic Numbers 73–83) as Measured with Magnetic Analysis. Observation angle was 90°.

particles emitted at various angles from various targets bombarded by 23-Mev protons were measured. The deuteron and triton angular distributions in all elements and the alpha angular distributions in heavy elements are strongly peaked forward; their energy distributions are peaked at high energy, in contrast to the situation in (d,p), (He^3,p), and (α,p) reactions. This can be explained by assuming that (p,d), (p,t), and (p,α) are pickup reactions which excite hole states; stripping reactions excite particle states. The (p,α) reactions on elements up to atomic number 50 have energy distributions of the type expected by a compound nucleus process. The energy spectrum shows evidence of a lower Coulomb barrier than that used to

explain experiments in which alpha particles bombard nuclei in their ground states. The (p,α) excitation functions and spectra at different bombarding energies are being obtained.

A study[3] of inelastic proton spectra from medium-weight elements as a function of bombarding energy revealed two maxima in the spectra which become quite distinct at some bombarding energies. An example of typical results is shown in Fig. 9. The most striking feature of these results is the double maximum consisting of one peak which occurs at about 5 Mev for E_B = 11.3 Mev and moves slowly to higher energies as E_B increases, and a second peak which first appears at about E_B = 14 Mev, rapidly increases in intensity, and moves to higher energies with increasing E_B until it fills in the valley between the two peaks above E_B = 17 Mev. This clearly suggests that two independent processes contribute to the spectrum, with one peak being due to each. The lower energy maximum can be explained as being due to "second protons" in a two-step evaporation process. If the spectra are decomposed into "first" and "second" protons, the spectra are explained by compound nucleus theory with a level density $w = \exp (aE)^{1/2}$ with a = 11 for r_o = 2.0 fermis, or a = 17 for r_o = 1.5 fermis.

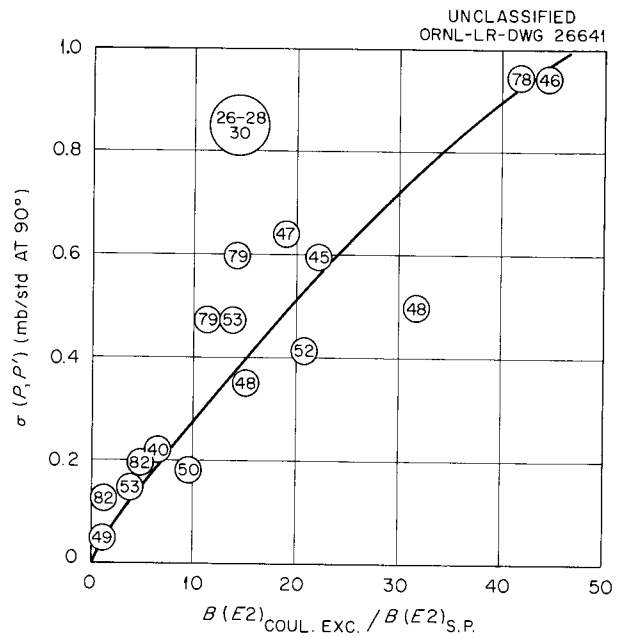

Fig. 8. Correlation Between Cross Sections for Exciting Given Levels by Inelastic Scattering of 23-Mev Protons (Ordinate) and Coulomb Excitation. Figures are atomic numbers of elements.

Elastic proton angular distributions from U^{235} and U^{238} and from 23-Mev proton fission cross sections for U^{233}, U^{235}, and U^{238} have been measured for a determination of optical model potentials. Also, elastic proton angular distributions from Ni^{64} and natural nickel have been measured

[3]B. L. Cohen and A. G. Rubin, Inelastic Proton Scattering in Medium-Weight Elements, submitted to Phys. Rev.

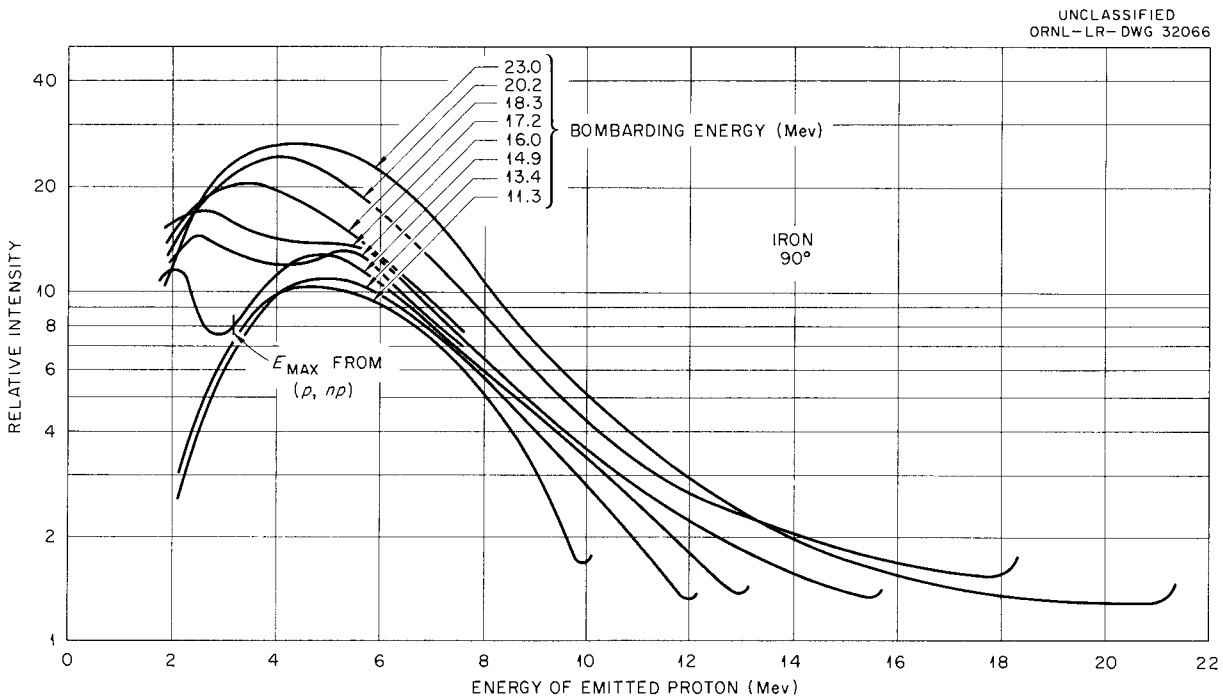

Fig. 9. Corrected Energy Spectra of Protons Emitted at 90° When Iron Is Bombarded with Protons of Various Energies.

to investigate a possible dependence of the real part of the potential on (N-Z)/A. This work is being extended and analyzed.

To study the sequence of nuclear levels excited in odd-A nuclei of the rare earths, enriched isotopes of erbium and ytterbium were irradiated with protons in the ORNL 86-Inch Cyclotron. Internal conversion electron studies[4] were made in the energy range of 8 to 1600 kev. The following activities were studied: Tm^{161} (~30 min), Ho^{161m} (E3, 211 kev), Tm^{163} (2 hr), and Lu^{167} (54 min), all previously unreported, as well as Tb^{161}, Ho^{161}, $Tm^{165,167}$, Yb^{167}, $Lu^{169,171,173}$, Hf^{173}, and possibly Yb^{169m} (E3, 24 kev). Genetic relationships and partial level schemes for decay chains are shown in Fig. 10. Data shown include those of Strominger[5] and Cameron.[6]

---

[4]B. Harmatz, T. H. Handley, and J. W. Mihelich, Nuclear Spectroscopy of Odd Mass (161-173) Nuclides Produced by Proton Irradiation of Er and Yb, submitted to Phys. Rev.

[5]D. Strominger, J. M. Hollander, and G. T. Seaborg, Revs. Modern Phys. 30, Part 2 (1958).

[6]A. G. W. Cameron, A Revised Semiempirical Atomic Mass Formula, AECL-433 (1957).

UNCLASSIFIED
ORNL-LR-DWG 32590R

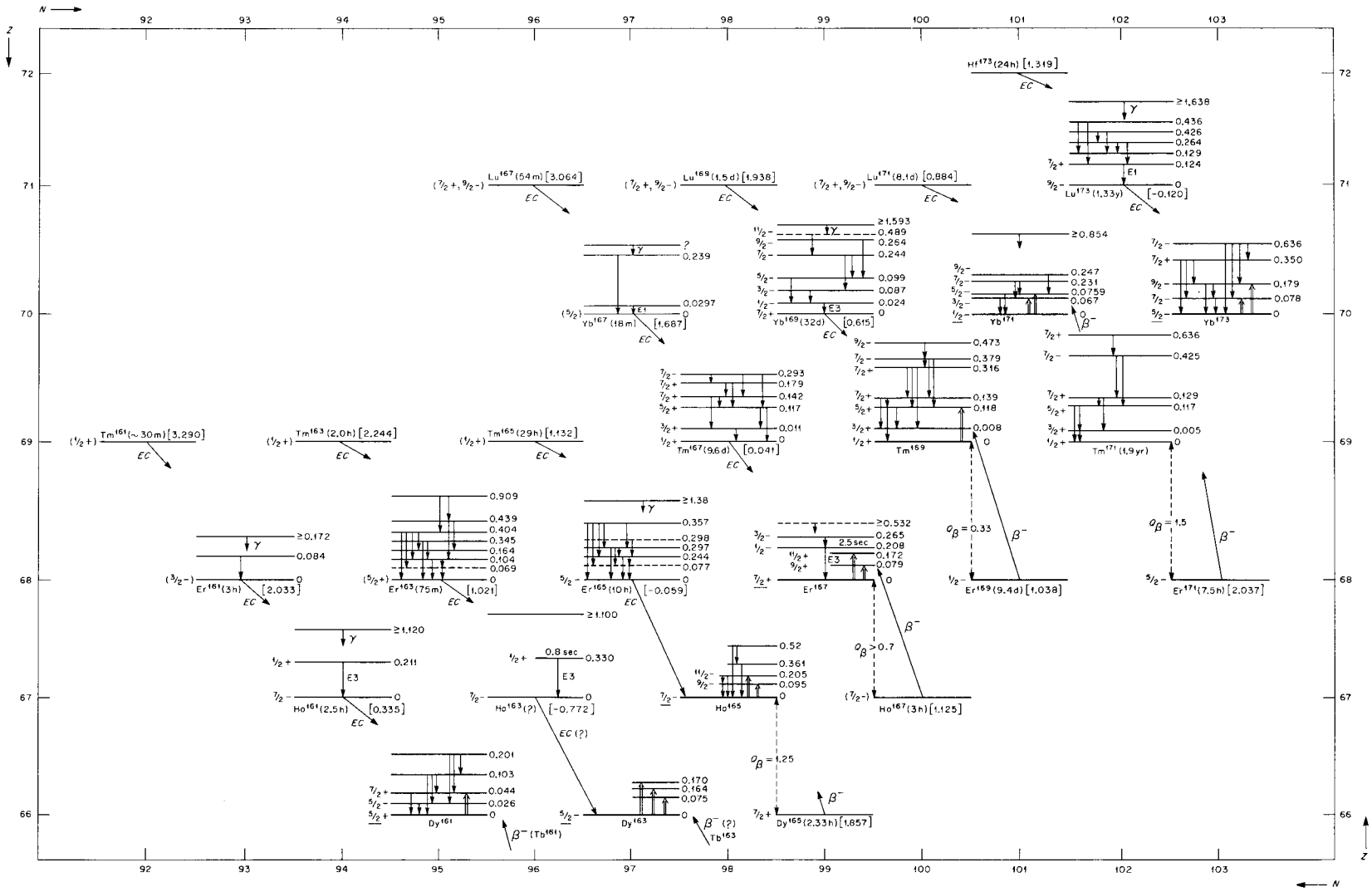

Fig. 10. Diagram Showing Genetic Relationship and Energy Levels of Odd-Mass Nuclei ($66 \leq Z \leq 72$) and ($92 \leq N \leq 103$). See text for explanation of vertical dashed lines and for figures in brackets.

No attempt was made to preserve an energy scale. The numbers in square brackets in Fig. 10 are the estimates of available energy (Mev) taken from the tables of Cameron. Energy differences between nuclei, where obtained from beta-decay studies, are indicated with vertical dashed lines. Where comparison is possible, excellent agreement with the predictions of the Copenhagen unified model is obtained, particularly for the case of the isotopes of Tb (Z = 65), Ho (Z = 67), and Tm (Z = 69), where striking similarities in the level structure are observed.

Applied Physics

Cyclotron time is made available for other research programs at this and other laboratories and for the production of isotopes for commercial processors.[7] Arrangements for service irradiations are made through the Applied Physics Group, which also maintains an active program of target development.

The number of radioisotopes produced in service irradiations for commercial concerns who handle the processing and distribution continues to increase. Cyclotron-produced radioisotopes added to the list include V^{48}, Ge^{68}, Rh^{102}, W^{181}, and Bi^{206}. Thirteen runs were made this year for the production of As^{74}, with a total yield of 1600 mc produced for cancer research. The production last year was 720 mc in eleven runs. Full yield data for these commercially produced isotopes are available, as summarized in Table 4.

Other radioisotopes produced in service irradiations for research programs in other laboratories but for which yield data are not complete were F^{18}, Ti^{44}, Y^{87}, Nb^{94}, Rh^{102}, Ce^{159}, Pm^{148}, Tb^{156}, $Au^{194,196}$, Au^{196m}, Hg^{197}, Pb^{202}, Bi^{205}, Bi^{206}, and Po^{209}. For other divisions of ORNL, F^{18}, Ga^{67}, Kr^{79}, Tc^{95m}, and Rh^{102} were made.

The problem of collecting a rare-gas product was solved in the production of Kr^{79}. Dependence on trapping the rare gas within the crystal lattice proved unsatisfactory. The capsule target was then modified for the collection of the off-gases. Yields obtained with this target were 1 to 2 orders of magnitude greater than for the vented capsule.

---

[7]Under the AEC full-cost recovery policy.

Table 4. Summary of Yield Data of Radioisotopes Produced for Commercial Distribution

Isotope	Reaction	Amount Produced (mc)	Runs	Production Rates (mc)		Target	Max Average Current (μa)	Max Hours Run
				Per Hour	Per Milliampere-Hour			
Be^{7}	Li^{7} (p,n)	204	2	22	108	Li cast on 6 × 5 5/8 in. Cu	200	5
V^{48}	Ti^{48} (p,n)	86	4	17	94	Capsule	185	2
Fe^{55}	Mn^{55} (p,n)	50	1	12	13	Mn plated on 6 × 5 5/8 in. Al	960	4
Co^{57}	Ni^{58} (p,pn) + (p,2n) + (p,2p)	50	1	25	27	Ni plated on 6 × 5 5/8 in. Cu	920	2
Ge^{68}	Ga^{69} (p,αn)	1.4	2	0.35	0.47	Capsule	185	2
As^{74}	Ge^{74} (p,n)	1600	13	14.3	75.4	Capsule	190	13
Sr^{85}	Rb^{85} (p,n)	142	5	3.8	18.8	Capsule	205	9
Y^{88}	Sr^{88} (p,n)	8.3	1	4.1	21.3	Capsule	195	2
Rh^{102}	Ru^{102} (p,n)	0.48	1	0.16	0.86	Capsule	185	3
Cd^{109}	Ag^{109} (p,n)	7.5	1	1.8	1.1	Ag plated on 6 × 5 5/8 in. Cu	1750	4
W^{181}	Ta^{181} (p,n)	18.3	1	6.1	7.5	Ta brazed on 6 × 5 5/8 in. Cu	815	3
Bi^{206}	Pb^{206} (p,n) + Pb^{207} (p,2n)	194	3	39	210	Capsule	195	3

The production of F^{18} continues at the rate of about one run per month for fluorine exchange studies by the Chemistry Division.

Three isotopes made for UCRL-Livermore are very long lived: Ti^{44}, $T_{1/2} = 10^4$ years; Nb^{95}, $T_{1/2} = 20{,}000$ years; and Pb^{202}, $T_{1/2} = 10^5$ years. Representative target techniques were used in the production of these isotopes. The Ti^{44} was produced by bombarding Sc_2O_3 in the capsule target, the Nb^{94} from zirconium metal soft-soldered to a copper flat-plate target, and the Pb^{202} from thallium metal cast into a depression in a copper flat-plate target.

Three zirconium foil stacks were bombarded for the Florida State University for the study of the $Zr^{90}(p,\alpha)Y^{87,87\underline{m}}$ excitation function.

Isotopically enriched targets were used in the production of Rh^{102}, Pm^{148}, and Tb^{156}. This procedure eliminates unwanted activities and increases the yield of the desired isotope.

Three shipments of $Au^{194,196}$, produced from a platinum foil bombarded in the window target, and one of $Bi^{205,206}$, produced from a lead plug bombarded in the capsule target, were sent to the Fysika Institutionen at Upsala, Sweden.

Zirconium is one of the new materials successfully fabricated into a flat-plate target. The technique used is to plate a thin (0.020-in.) sheet of zirconium on one side with nickel to a thickness of 0.001 in., heat the plated sheet in an inert atmosphere to outgas and to obtain a diffusion bond between the nickel and zirconium, and then soft-solder it to a copper back-plate. One such target was successfully operated at 500 μa.

Both lead metal and gallium metal were successfully run in the capsule target. The yields of Bi^{205} and Bi^{206} from the lead target are 65 and 265 mc/ma-hr, respectively. Even though the yield in mc/hr is reduced a factor of 20 over those from flat-plate targets, the capsule target is cheaper and much easier to prepare and process, and so there are definite advantages to using it. The gallium metal was run successfully in a nickel capsule; an aluminum capsule containing gallium rapidly disintegrated.

The development of a target for the production of Ca^{47} by the reaction $Ca^{48}(p,pn)Ca^{47}$ has continued. Difficulties in the production of a

thin calcium metal target led to the consideration of calcium compounds — in particular CaF_2. Three successful runs of CaF_2 vacuum-evaporated onto aluminum have been made, but only one of these has been analyzed to date. The yield was 0.04 mc from 413 mg of natural CaF_2 in a 4-hr run, that is, 10 μc/hr from 215 mg of natural calcium. This value is not in disagreement with the yield reported from a natural-calcium metal target in the last annual report.

In addition, four runs in which a mixture of beryllium and titanium was bombarded in the capsule target were made in a search for Ca^{47} produced by the $Ti^{50}(n,\alpha)Ca^{47}$ reaction. Beryllium was used both as a powder and as a plug and the titanium as metal powder and TiO_2. There was no Ca^{47} seen in any of the four targets after a 4-hr bombardment at 200 μa.

ELECTRONUCLEAR MACHINES

Development and application of the concept of an azimuthally varying magnetic field[1] (AVF) were undertaken in 1950–1952 to provide high currents in the ORNL 86-Inch Cyclotron. When the performance goals were achieved with a conventional field, the problem lost its urgency.

Active interest in the development of the AVF cyclotron was renewed in late 1954, and an extensive theoretical study of the properties of machines of this type was begun. Analytical studies of ion orbits soon indicated possible resonance problems, and so, at an early stage, numerical integration procedures were devised and coded for the digital computer so that orbit behavior in complex fields could be studied in precise detail. These theoretical studies and development tests led to the proposal[2] for a high-energy accelerator installation incorporating an AVF fixed-frequency cyclotron to accelerate protons to ~850 Mev.

Continued theoretical work has included studies of the fundamental acceleration process, the focusing properties of the fields, the effects

---

[1] L. H. Thomas, Phys. Rev. 54, 580–98 (1938).

[2] F. T. Howard et al. (eds), Proposal for a Southern Regional Accelerator, ORNL CF-57-4-30 (April 1957).

of nonlinearities and resonance difficulties, the effects of factors which determine beam quality, and details of deflection systems appropriate for such devices.

In addition to these theoretical studies, an operating relativistic AVF cyclotron was constructed for the purpose of experimentally verifying the various computations. This device, known as Cyclotron Analogue I (CA-I), accelerates electrons to a velocity of 0.7 c (in units of velocity of light) and to a radial focusing frequency of 2 (in units of the orbital frequency). The magnetic field in the CA-I is of a four-sector radial configuration. The field is obtained from a precisely fabricated set of air-cored coils, the detailed performance of which was completely and accurately precalculated. In operation, CA-I has strikingly verified the design calculations, particularly those on the crucial question of resonance behavior, and thus has demonstrated the complete feasibility, from an orbit dynamics standpoint, of the AVF cyclotron.

A second analogue having a spiral magnetic field configuration is being designed for studying in more detail the performance of the proposed 850-Mev cyclotron. This unusual cyclotron would be used to inject large proton currents into a proton synchrotron. For use in studies of high-energy injection the electron analogue of the Brookhaven 25-Gev Alternating-Gradient Synchrotron was acquired and moved to the Laboratory. After the completion of further theoretical studies the Synchrotron Analogue will be installed for extensive experimental work.

Cyclotron Analogue I

Cyclotron Analogue I is a fixed-frequency cyclotron in which electrons are accelerated to an energy of 190 kev in an azimuthally varying magnetic field with fourfold periodicity. The details of the CA-I design and the early experimental work were given in previous reports.[2,3] During the early part of the present period, much of the earlier experimental work was repeated, and the measurements were refined. A summary

---

[3]Electronuclear Research Ann. Prog. Rep. Oct. 1, 1957, ORNL-2434, p 21.

report[4] covering theory, design, and experimental results has been published. Additional experimental work completed since the last report is reviewed in the following paragraphs.

Resonances. — A new survey of resonances between the radial and axial focusing frequencies, ν_r and ν_z, was completed with an improved electron source and with more accurate calibration of the detector position. The new results support the data reported previously, and the assignments for the coupling resonances $\nu_r - \nu_z = 1$ and $2\nu_r + 2\nu_z = 4$ (or $\nu_r + \nu_z = 2$) were definitely established. The assignments were made by determining the radial position of the resonance and the direction and magnitude of the change in radial location of the resonance produced by a fixed change in flutter (which changes ν_z). Table 5 summarizes the results. The assignment for the resonance at r = 28.81 cm is $2\nu_r + 2\nu_z = 4$ rather than $\nu_r + \nu_z = 2$, because the former is an essential linear resonance, while the latter is an imperfection resonance which would require a second harmonic error in the magnetic field.

Table 5. Location of $2\nu_r + 2\nu_z = 4$ Resonance

Flutter (f_o*)	Calculated Value (cm)		Observed Value (cm)	
	r	Δr	r	Δr
1.01	28.64	0.17	28.70	0.15
1.00	28.81	0.11	28.85	
0.99	28.92		28.97	0.12

*f_o is the design value of the flutter.

Threshold Measurements. — All fixed-frequency cyclotrons have a voltage threshold, that is, an accelerating voltage below which the particles cease to be accelerated to the final radius. This is caused by loss of synchronism between the frequency and the accelerating voltage frequency to the extent that at some point the relative phase becomes

[4]H. G. Blosser et al., Rev. Sci. Instr. 29, 819–34 (1958).

$\pi/2$ radians, and the voltage gain per turn is zero. Lack of exact synchronism results because of magnetic-field errors; for a given error, the total phase shift depends linearly on the number of orbit turns and thus inversely on the accelerating voltage.

The earlier measurements in CA-I yielded a figure of 140 ev/turn, which indicated that the electron made ~1300 revolutions to reach full energy. Our latest measurement indicates that the threshold is about 85 to 100 ev/turn and that about 2200 turns are made. The indicated mean-field accuracy from the later measurement is about 1/8000, which is what was expected from construction accuracy of the machine.

To further verify the validity of the threshold measurements, time vs accelerating voltage was measured. The results, plotted in Fig. 11, indicate constant average phase. It might be expected that the curves would show a gradually decreasing slope as the threshold is approached. Data are plotted for both the $\nu_r = 2$ and the $\nu_r = 4/3$ resonances. Also plotted for reference are lines calculated from the known energy for the two points, 190 and 104 kev, respectively, and from the measured voltage gain per turn. That these lines differ from the time measurements must indicate that either the average phase is different from zero and is constant or that there is an error in voltage calibration. The latter is much more likely. The indicated voltage error of 10% does not take into account the possible variation of voltage along the lip of the dee. It may be that the threshold is nearer 100 rather than 85 ev/turn.

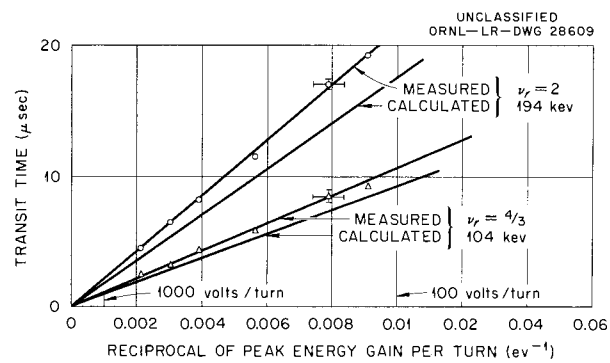

Fig. 11. Variation of Transit Time with Energy Gain.

The finding that the average phase remains relatively constant suggests that the threshold may be limited by some effect other than lack of isochronism. Axial defocusing or lack of sufficient radial focusing at the center of the machine would lead to substantial beam loss at low energy gain per turn. The fact that the threshold is essentially independent of final energy from well inside $\nu_r = 4/3$ to full energy supports the suggestion that a central region effect is being observed.

Focusing Frequency. – In CA-I the vertical focusing frequency, ν_z, is essentially constant at about 0.18; however, the radial focusing frequency, ν_r, increases monotonically from 1.0 at the center to the value 2.0 where acceleration ends because of radial blow-up of the beam. Early measurements of the radial focusing frequency deviated substantially from the predictions obtained by detailed orbit integration with the Oracle (see Fig. 12).

In brief outline, the method of measuring ν_r consists of inserting into the beam a probe, the tip of which is excited by a variable-frequency r-f oscillator. The probe tip is arranged to produce an essentially radial electric field through which the beam passes. If the frequency of the oscillator is then tuned to the frequency of free radial oscillation, a disturbance should be noted. This method was used in both the early and recent experiments; however, a number of refinements and improvements in technique were added.

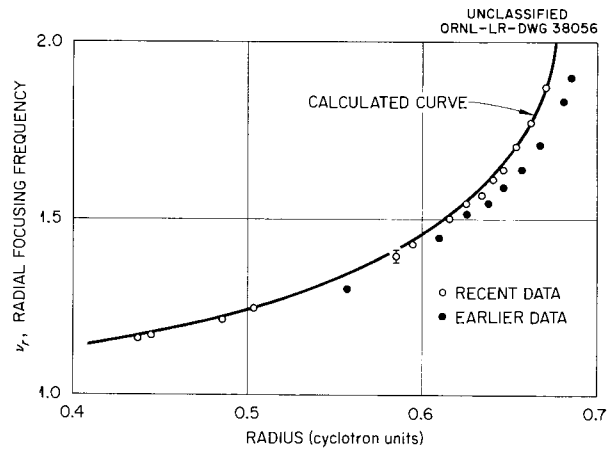

Fig. 12. Measurements of Radial Focusing Frequency, ν_r.

The following improvements were made to afford greater sensitivity and to make the radius of measurement agree with the radius of the disturbance: An improved electron gun was used which gave perhaps a factor of 10 more current per pulse; the photomultiplier tube was coupled to the oscilloscope through a cathode-follower circuit which reduced the observed pulse width by a factor of 2; the knockout-oscillator tip was modified to block the beam and to thus eliminate a screening probe referred to in the previous paragraph.

The new measurement technique was as follows: (1) At approximately the desired radius of measurement, a small beam was obtained with the dee voltage only 10 to 20% above threshold. (2) The knockout-oscillator probe was moved in until essentially 100% of the beam was intercepted on

its tip. (3) The detector was advanced until 30 to 50% of the original beam was observed. (4) The knockout oscillator was tuned until an effect on the received pulse was noted, and the knockout-oscillator voltage was reduced until an effect was barely observable. If possible, the dee voltage was reduced still further. The effect observed was, rather than an increase in pulse height, a decrease in pulse height and a broadening toward shorter times, indicating that some particles were reaching the probe tip from inner orbits through radial oscillation rather than acceleration. The shift in time was at most 0.05 μsec (observed on 0.2 μsec/cm sweep speed). This placed an upper limit on the error in radial position of about 0.001 cyclotron unit (0.04 cm). The results of the new measurements are also shown in Fig. 12.

Electron Injector. — Conventional electron sources for CA-I such as the filamentary type or the secondary emission type, which depend upon the dee voltage for extraction, give a beam of large radial oscillation amplitude. This is most apparent at the $\nu_r = 4/3$ resonance, where ~75% of the beam blows up radially while the remainder, originally of small radial amplitude, accelerates smoothly through the resonance. It can be shown theoretically that the radial oscillation amplitude depends on the detailed starting conditions. This has also been demonstrated experimentally by noting that the resonance transmission depends on the exact position of the source, and can be varied over wide limits by application of constant voltage to the source.[3]

To observe the transmission through the $\nu_r = 4/3$ resonance under better controlled conditions, an injector-type electron source was developed which directs a narrow beam of 3.1-kev electrons into the machine at the appropriate radius. Figure 13 shows a schematic of the injector. Electrons are accelerated through a narrow slit into a 180° analyzer section at +500 v. The angular width of the beam is reduced to ±1/2°. The 0.005-in. exit slit of the analyzer section provides momentum analysis. After passing through the analyzer, the electrons gain an additional 2.6 kev in passing across the exit gap. The angle of emission of the source is adjustable to enable placing the beam on the equilibrium orbit. Figure 14 is a photograph of the source under test between a pair

of Helmholtz coils in a test chamber. The beam of small radius is spurious and is produced by secondary electrons from the final analyzer slit being accelerated across the exit gap.

The qualitative results obtained with the injector are gratifying. Substantially 100% transmission through the $\nu_r = 4/3$ resonance is achieved. The transmission is very sensitive to source angle and voltage, as expected.

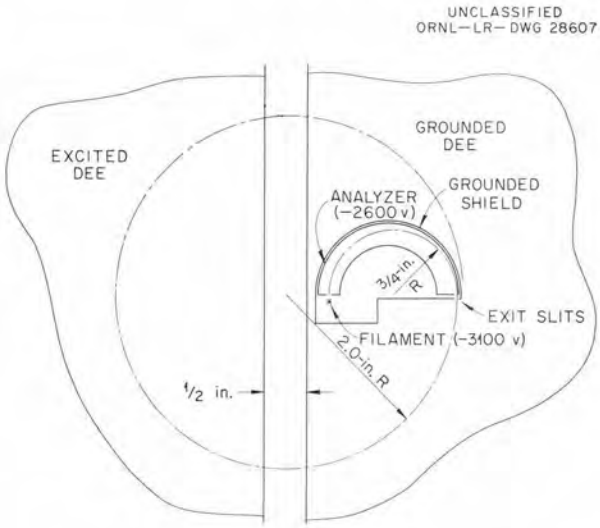

Fig. 13. Injector-Type Electron Source.

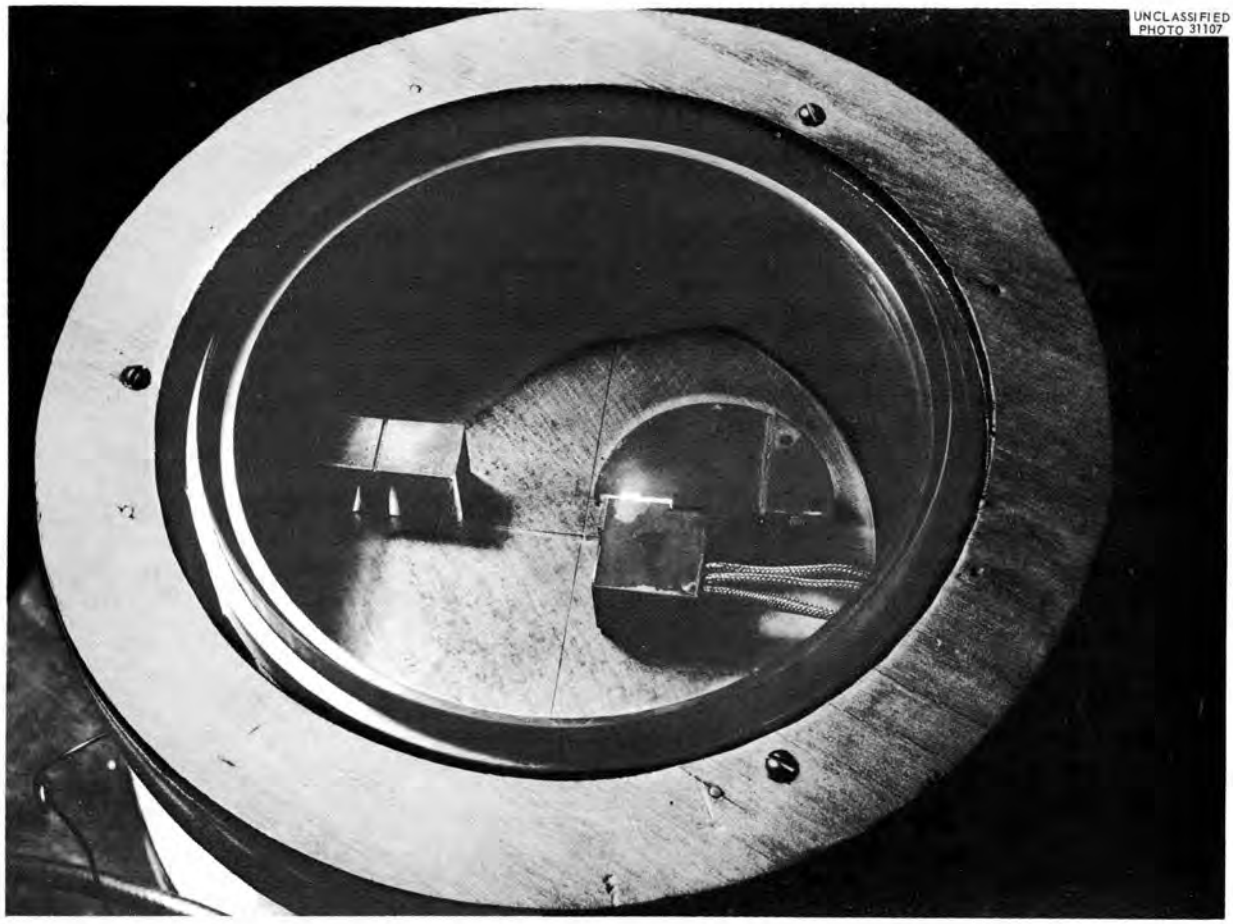

Fig. 14. Injector-Type Electron Source in Test Chamber.

Cyclotron Analogue II

Cyclotron Analogue II (CA-II) is a fixed-frequency electron cyclotron with a spiral eight-sector azimuthally varying magnetic field designed to provide axial focusing and constant orbit period for energies well beyond the $\nu_r = 8/4$ resonance. The introduction of a spiral configuration of the magnetic field sectors reduces the degree of azimuthal variation required and also increases the energy at which the integral resonance occurs.

CA-II models the beam dynamics of the 850- to 900-Mev proton cyclotron proposed as the injector for an ~10-Gev alternating-gradient synchrotron.[5] CA-II will be used primarily to study beam extraction at the $\nu_r = 4/2$ and $8/4$ resonances. The machine is being designed so that the feasibility of passage through the $\nu_r = 2/1$, $4/2$, and $8/4$ resonances (which occur at the same energy) can also be studied.

A brief tabulation of the properties of the machine follows:

Cyclotron unit (c/ω)	16,000 in.
Central field (B_0)	41.926 gauss
Rotational frequency	117.399 Mc/sec
Axial focusing frequency, ν_z	0.2
Energy for $\nu_r = 8/4$	~470 kev
Maximum energy	~510 kev

The magnetic field at a point on the median plane can be expressed as follows:

$$B(r,\theta) = \overline{B}(r) \left[1 + \sum_{n=1}^{\infty} f_n(r) \cos 8n\,(\theta - \xi) \right] ,$$

where θ is in radians, and the unit of length (r) is the cyclotron unit, c/ω. The spiral angle of the magnetic field is given by $\xi = r^2$. This choice minimizes the higher order derivatives of the spiral angle, which influence the stability of orbits at high energy.

---

[5]F. T. Howard et al. (eds), Proposal for a Southern Regional Accelerator, ORNL CF-57-4-30 (April 1957).

Magnetic-Field Design. — The coil design was outlined in considerable detail in the last progress report.[6] Since that time it has been found necessary to considerably revise the coil shape because the spiral of the field deviated considerably from the desired function $\xi = r^2$. These deviations were not apparent earlier because of the order in which the calculations must be carried out. The simplified smooth approximation formula for the axial focusing frequency is used in making the initial design of the magnetic field:

$$\nu_z^2 = - \frac{r^2}{1 - r^2} + \tfrac{1}{2}f^2 \quad (1 + 2 \tan^2 \gamma) \quad .$$

In designing the field it is customary to assume that $\tan \gamma$ is as specified and then to determine the r dependence of the term $(\frac{1}{2}f^2)$ for the desired value of ν_z. A set of coils is then developed which produces the desired flutter. For this purpose an Oracle calculation determines the value of $\frac{1}{2}f^2$ according to the following approximate formula:

$$\tfrac{1}{2}f^2 = (\overline{B^2} - \overline{B}^2) \; (1 - r^2) \quad .$$

The result may be used to calculate ν_z (r) for the particular coil set.

The first design, previously reported, produced the desired flutter variation with radius but, unfortunately, because of the method of specifying the end points of the coil segments, produced a magnetic field which did not follow the desired $\xi = r^2$ spiral at large radii. The end points of the coil were placed symmetrically along the perpendicular to the radius vector at the point on the center of the coil. Figure 15 shows a comparison between the orbit properties calculated from the smooth approximation and those determined by precise numerical orbit integration. Some of the fine structure is a result of the interpolation routine in the orbit code; however, the general character is as shown. The large deviation of ν_z from the prediction of the smooth approximation is a result of spiral angle deviation from the desired function.

---

[6]Electronuclear Research Ann. Prog. Rep. Oct. 1, 1957, ORNL-2434, p 25.

To correct this difficulty, a new scheme for coil specification has been adopted in which the end points of the coil segments are specified symmetrically along the normal to the $\zeta = r^2$ curve at the point in question rather than along the normal to the radius vector at the point as previously done. Also, for ease and precision in fabrication, an additional change was that the coils should be composed of a series of tangential arcs rather than straight-line segments. A new Oracle program was written which computes the magnetic field of circular arc sectors with general location orientation, included angle, and current sense. In preliminary design, the circular arcs are approximated by a series of straight-line segments to reduce computation time. Figure 16 shows the new shape that was developed.

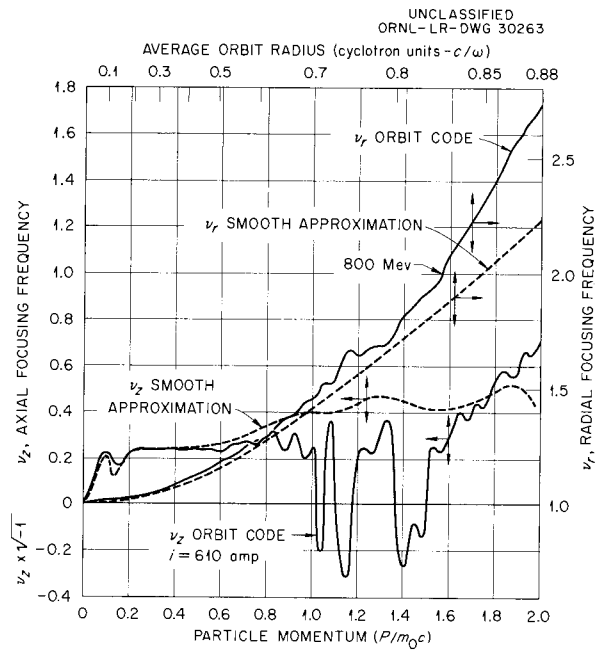

Fig. 15. Orbit Properties for CA-II.

The fitting problem has not yet been completed with the new criteria; however, considerable progress has been made. Figure 17 shows the required flutter curve for $\nu_z = 0$, 0.2, and 0.5, with the results for a preliminary coil set superimposed. Figure 18 shows the results for the orbit integration using the same fields; the agreement with the smooth approximation is much better than that obtained previously.

The flutter coil set contributes appreciably to the average field. The residual field which must be supplied by the main average-field coil set is of rather irregular shape. Preliminary fitting attempts show that the field shape over most of the machine can be produced alternately by a set of several coils located 0.2 cyclotron unit (3.2 in.) from the median plane beginning at r = 0.5 and spaced radially 0.1 cyclotron unit. Additional windings will compensate for the hump in the field produced by the tip of the sector coils at the center of the machine. Final average

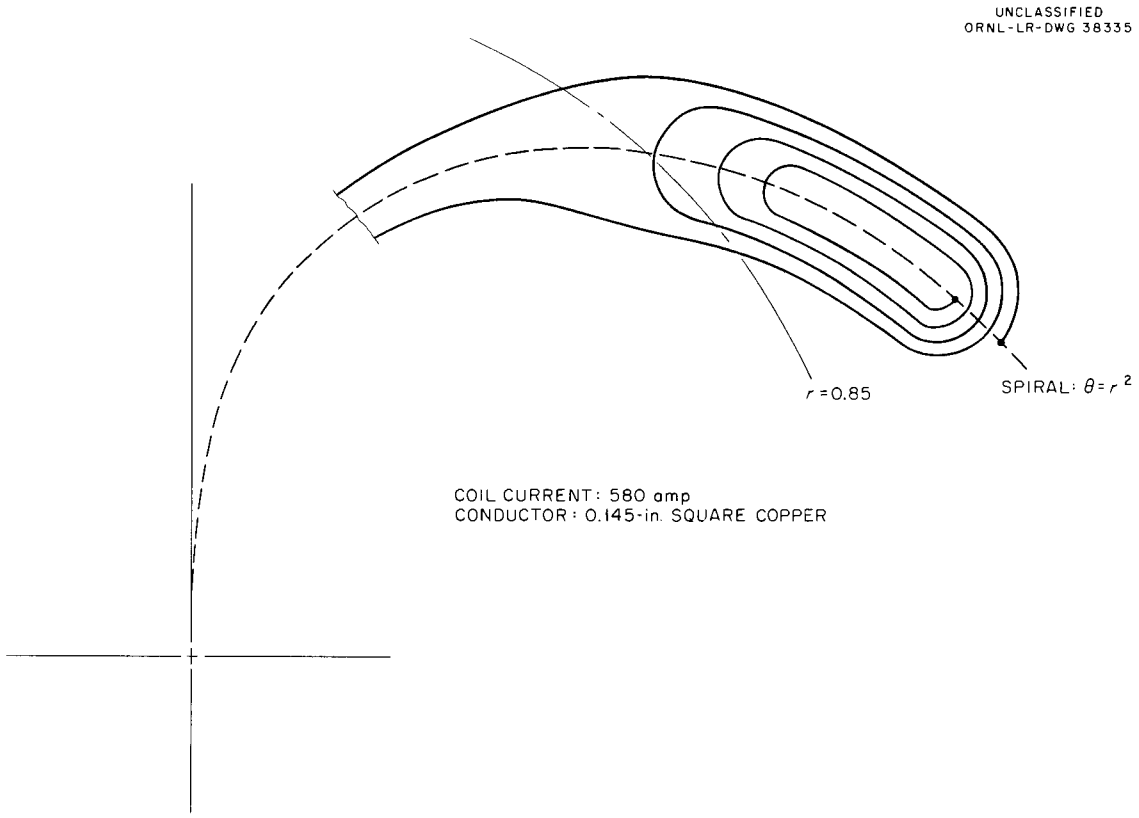

Fig. 16. Sector Coils for CA-II.

field fitting will be provided by a set of circular trimming coils located approximately 0.05 cyclotron unit from the median plane.

Coil Fabrication. – The sector coils to produce the spiral magnetic field of CA-II pose a difficult design problem. The use of relatively fine wire, as in the CA-I coils, is ruled out because of the concave curvature of one side of the coil. The most attractive method involves the use of only a few turns of heavy conductor carrying a current of approximately 600 amp (see Fig. 16). Precision and cooling requirements have required the development of unusual fabrication methods. The square tubing originally considered has been tentatively rejected because of the very high precision required of the hole location; also the distortion at the cross section at bends would be excessive.

A new scheme receiving consideration is the bonding of rectangular, uninsulated copper to an anodized aluminum plate provided with water passages. The ~0.0002-in.-thick anodized layer provides the electrical insulation. Adequate heat transfer and close mechanical tolerances can be

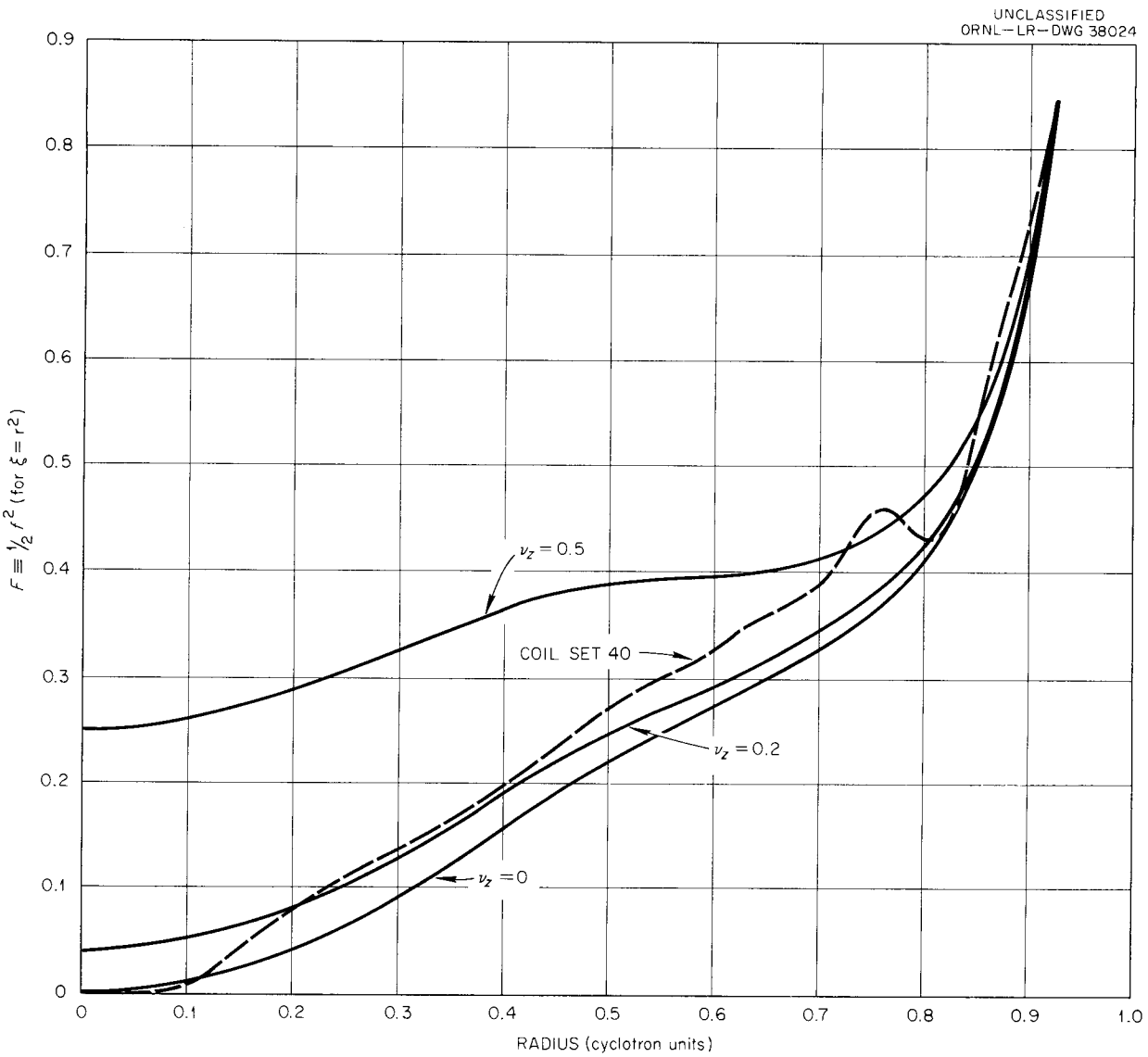

Fig. 17. Flutter of Preliminary Coil Set, CA-II.

achieved with this system. The use of current density as high as 30,000 amp/in.^{2} seems feasible. The close lateral tolerances (0.001 in.) can be achieved by locating the conductor in a master die during bonding.

Figure 19 is a photograph of a test assembly consisting of a section of 1/8-in. square copper conductor bonded with Eastman 910 cement which has good smear and tensile strength properties at temperatures in excess of 100°C. At 450 amp (29,000 amp/in.^{2}) the temperature rise in this particular coil was only 5°C.

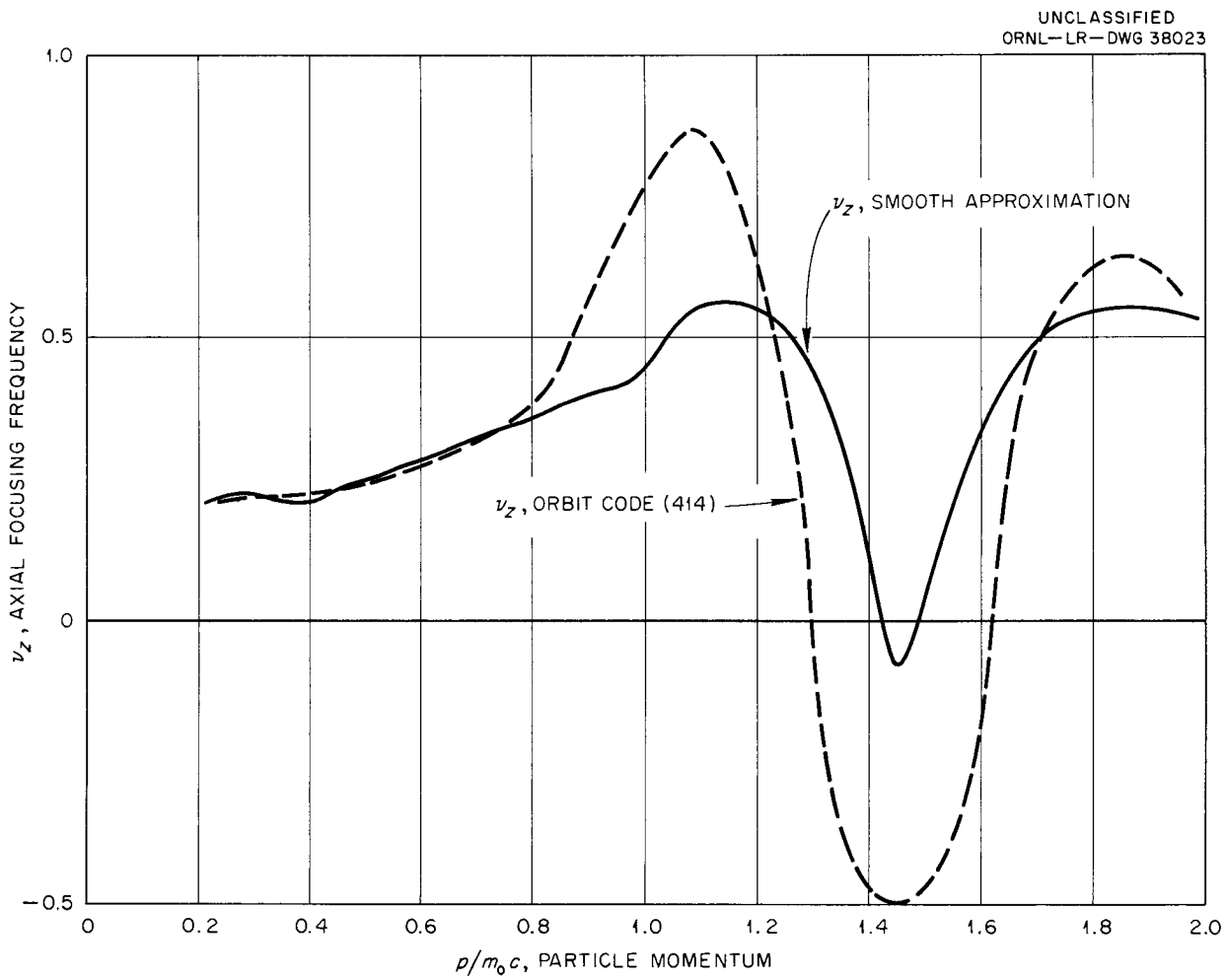

Fig. 18. Axial Focusing, ν_z, as Calculated by Orbit Code and by Smooth Approximation.

Precision Requirements. — A systematic study of the effect of fabrication errors was made for the original coil design. The results are expected to be fully applicable for the new coil configuration. Small segments of each coil were moved 0.010 in., and the resultant changes in the average field and flutter were noted. The results indicate that the required accuracy of the average field is the controlling factor; a precision of ±0.001 in. will be required in conductor location. When the redesign of the sector coils by the new procedures is completed, the mechanical tolerance situation will be re-examined.

UNCLASSIFIED
PHOTO 32562

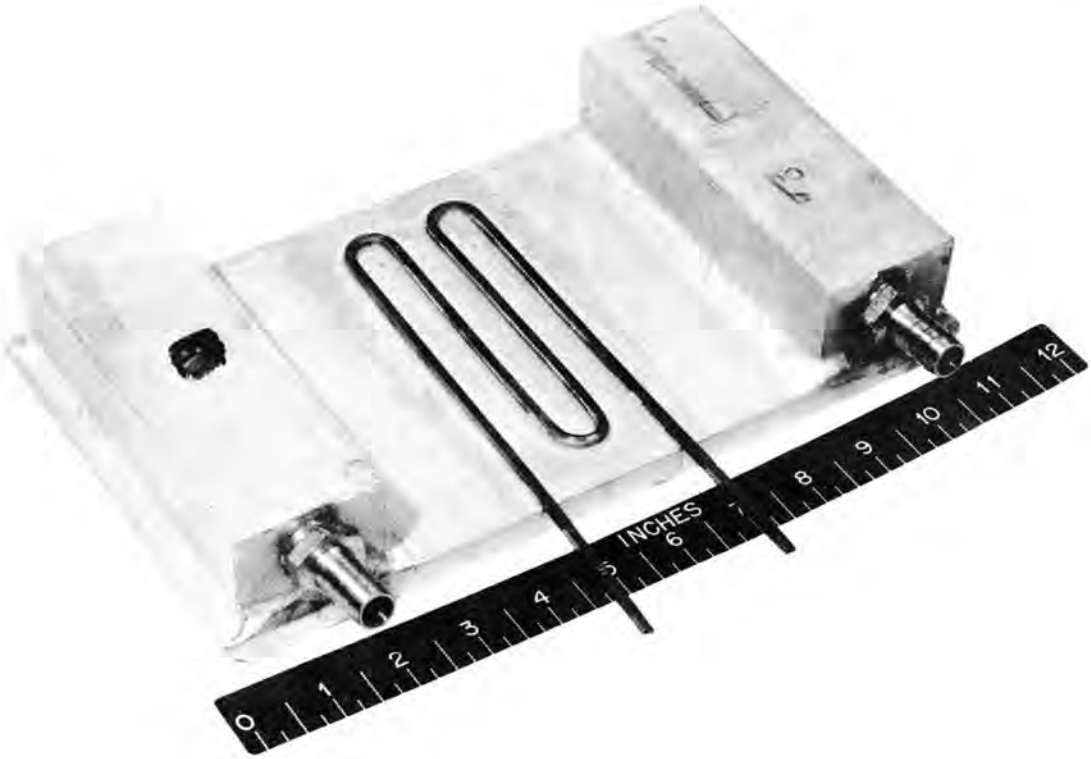

Fig. 19. Test of Coil Fabrication Scheme for CA-II.

Vacuum Chamber. — The design requirements for the vacuum chamber and coil supports for CA-II are quite similar to those for CA-I; however, the closer mechanical tolerances will require minimizing accumulative assembly errors. Also, the high current leads to the sector coils will require precise mounting, and in some cases coaxial leads will be required. Present plans are to use an octagonal vacuum chamber of substantially smaller volume than that of CA-I. Large rectangular windows are planned which will allow easy access and greater flexibility. As in CA-I, the vacuum system will consist of two parts: a mechanically pumped system containing the coils, and a high-vacuum system (10^{-6} mm Hg) for the dees and beam space. The two systems are separated by 1/16-in.-thick plates.

R-F System. — The initial design of the CA-II r-f system consisted of quadrant-type resonators operating at twice the cyclotron frequency. However, it has since been found advisable to provide a third-harmonic accelerating voltage and to regulate the r-f voltage in order to obtain optimum beam deflection in the machine. Since the addition of a third harmonic to the quadrant resonator did not appear feasible, it was decided to construct a single-dee r-f system.

As mentioned previously, it will be necessary to regulate the r-f accelerating voltage. A proposed closed-loop system for accomplishing this is shown in block diagram (see Fig. 20). The transmitter power-amplifier plate and screen voltages will be supplied from regulated power supplies whose outputs are controlled by an error amplifier. The input to the error amplifier will be the difference between a d-c reference voltage and the rectified output of the transmitter. This secondary loop will be incorporated in another loop containing the accelerating electrode, the dee. It should be possible to obtain at least a 0.1% short-term regulation with this system; however, the long-term regulation, or drift, would probably be poor since absolute measurement of a VHF voltage to 0.1% is extremely difficult.

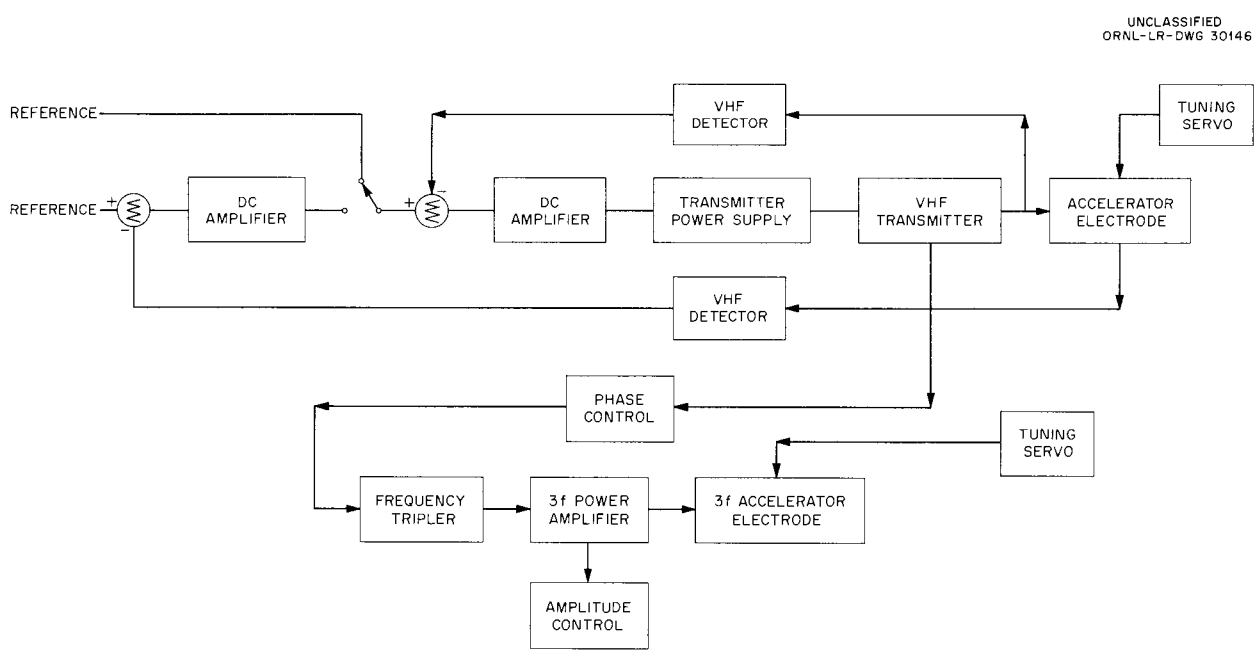

Fig. 20. Block Diagram of R-F System for CA-II.

The phase control for the third harmonic will consist of a coaxial "line stretcher" between the transmitter and frequency tripler. At present, servo control of the phase is not planned; however, it may be added later, if necessary. The amplitude control for the third harmonic will be a closed-loop regulator quite similar to that described for the fundamental except that the regulation may be less precise.

THE OAK RIDGE RELATIVISTIC ISOCHRONOUS CYCLOTRON

The Oak Ridge Relativistic Isochronous Cyclotron (ORIC) is an outgrowth of the research programs with two cyclotrons built at Oak Ridge, the ORNL 86-Inch and the ORNL 63-Inch Cyclotrons. These machines, largely improvised from existing equipment, have contributed to the field of proton and heavy-particle physics, respectively.

Construction of a new cyclotron was originally proposed by the Laboratory to free the heavy-particle experimental program from the handicaps of the physical environment of the 63-in. cyclotron and, by increasing the particle energy, to open up the upper two-thirds of the periodic table as possible experimental territory. In 1955 the Laboratory proposed that a replacement cyclotron, designated the 48-in., be constructed to permit heavy-ion physics to continue under somewhat improved circumstances in an adjunct to Building 9201-2 at Y-12. In 1957 the Commission approved this project to the amount of $459,000. The designs for the cyclotron components were prepared and orders were placed for the magnet steel and conductor.

In the meantime there has been an increasing interest in more precise work in the intermediate-energy field. Attention has been focused on the improvement of the fixed-frequency cyclotron. Efforts have been directed especially toward overcoming the limitations of energy imposed by the relativity effect, on providing great flexibility in the choice of both energy and the particle to be accelerated, on improving the energy definition, and on increasing the beam current and stability.

Advances in cyclotron technology have been made at a steady rate. Studies of properties of ion orbits (for high-energy particles) have shown the improved performance possible with alternating strong and weak sections in the magnetic field. The accurately predictable performance of the CA-I supported these theoretical studies. Accelerating protons to 75 Mev in a fixed-frequency cyclotron, previously impossible, has now become relatively straightforward. New systems for varying the radio-frequency offer the possibility for continuous variation of the energy for a wide choice of particles. New ideas for control of radial oscillations and r-f amplitude indicate that beams of much finer definition are possible.

In the face of these technological developments the design features and performance goals for the 48-in. cyclotron were re-examined. It was found that the new magnet, being fabricated, could be adapted to the design of a much more modern and versatile cyclotron. The concept of the ORIC was then advanced as a replacement for both the 86- and the 63-in. cyclotron and as an alternate to the 48-in. one.

Many new features have been incorporated in the ORIC to provide the full research potential which now appears practicable for a fixed-frequency cyclotron in the intermediate energy field: an azimuthally varying magnetic field (AVF) to provide axial focusing; an average magnetic field increasing with radius in a manner to keep the accelerated particle approximately synchronous, thus to minimize the threshold voltage required; an oscillator adjustable through an extended range, 3:1, of fixed frequencies; harmonic acceleration to provide additional bands of frequencies; auxiliary coils of various types to control the magnetic field configurations within a wide range of average field strengths; defining grids near the center to eliminate components of the beam with radial oscillations of large amplitude; and r-f amplitude control to reduce the energy spread in the beam.

The detailed model magnet measurements, the extensive orbit calculations, the preliminary studies of possible radio-frequency systems, the investigations of beam quality and deflection problems, and the other work basic to the development of a feasible cyclotron design have recently been

summarized in a separate document.[1] Material is presented here only to provide a brief description of the machine and the anticipated performance.

Anticipated Performance. — The ORIC is a variable-energy, azimuthally-varying-field, 76-in., fixed-frequency cyclotron designed to accelerate various particles with e/m ratios from 1 to 0.125 over a wide range of energies, up to 145 Mev. The machine is designed to accommodate large ion currents, with a total beam power up to 75 kw (1 ma of protons at 75 Mev). The conditions associated with the acceleration of various particles to their maximum respective energies are listed in Table 6 and presented graphically in Fig. 21.

Design Characteristics. — The most conspicuous features of the ORIC are shown in a photograph of the model, Fig. 22. The three-sector magnet pole, with slight spiral, is shown at the left. A pole tip with its various special windings is shown in Fig. 23. The azimuthally varying field

---

[1]R. S. Livingston and F. T. Howard, The Oak Ridge Relativistic Isochronous Cyclotron, ORNL-2648 (Sept. 1958).

Table 6. Conditions Under Which Various Particles May Be Accelerated in ORIC

	Charge State	Max Energy (Mev)	Energy per Nucleon (Mev)	Orbital Frequency (Mc/sec)	Central Magnetic Field (kilogauss)
Proton	+1	75	75	22.5	14.8
Deuteron	+1	39	19.5	12.3	14.5
He^3	+2	100	34	15	14.7
Alpha	+2	78	19.5	12.3	14.5
C^{12}	+4	115	9.5	8.6	17
N^{14}	+4	100	7.3	7.5	17
O^{16}	+4	88	5.7	6.5	17
Ne^{20}	+5	108	5.7	6.5	17
A^{40}	+7	103	2.8	4.6	17
Kr^{84}	+12	145	1.8	3.7	17

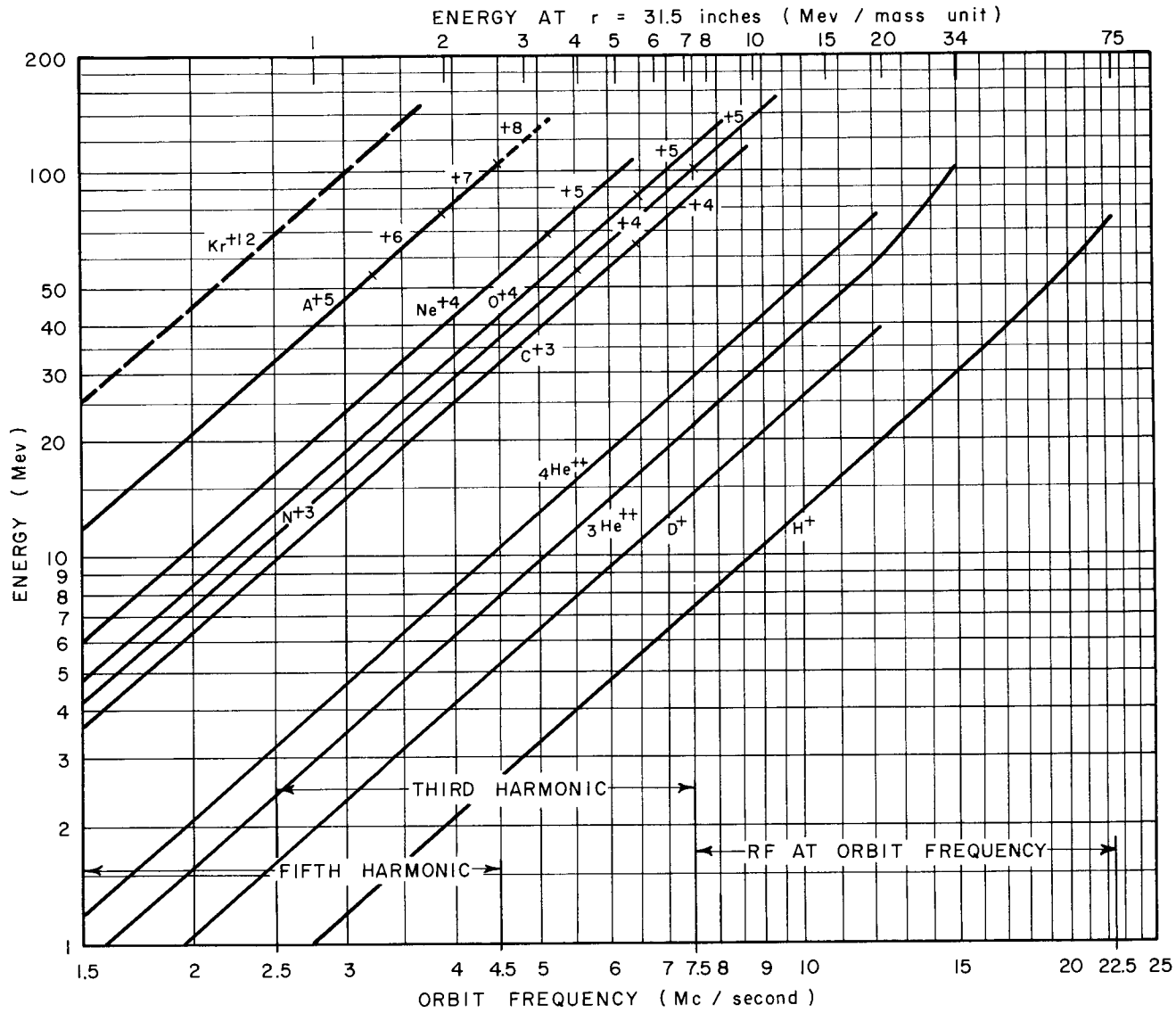

Fig. 21. Accelerated Particles and Energies Available in the ORIC.

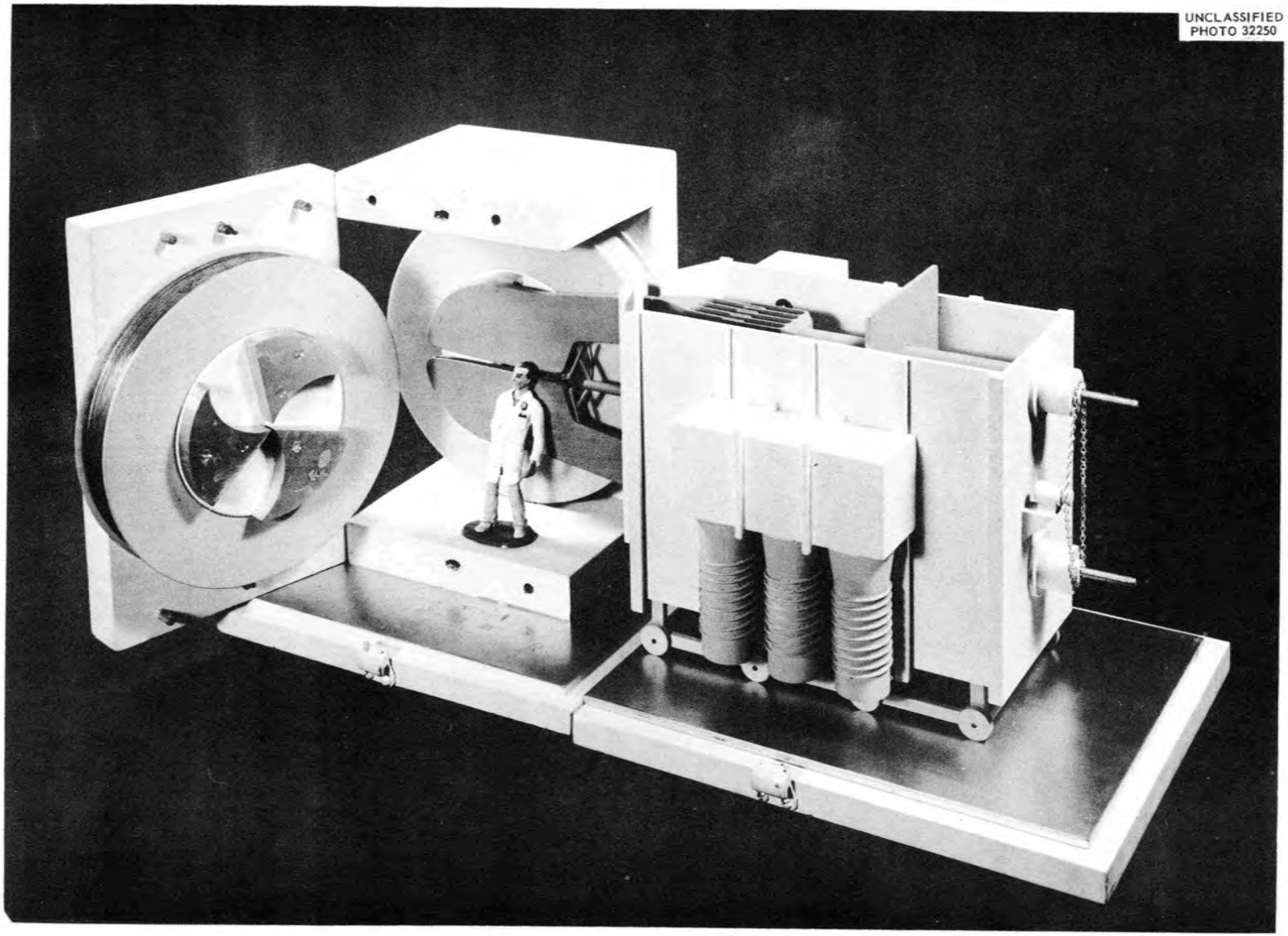

Fig. 22. Model of the ORIC Showing the Three-Sector Magnet Pole Tips and the Dees with One of the Resonant Circuits Studied.

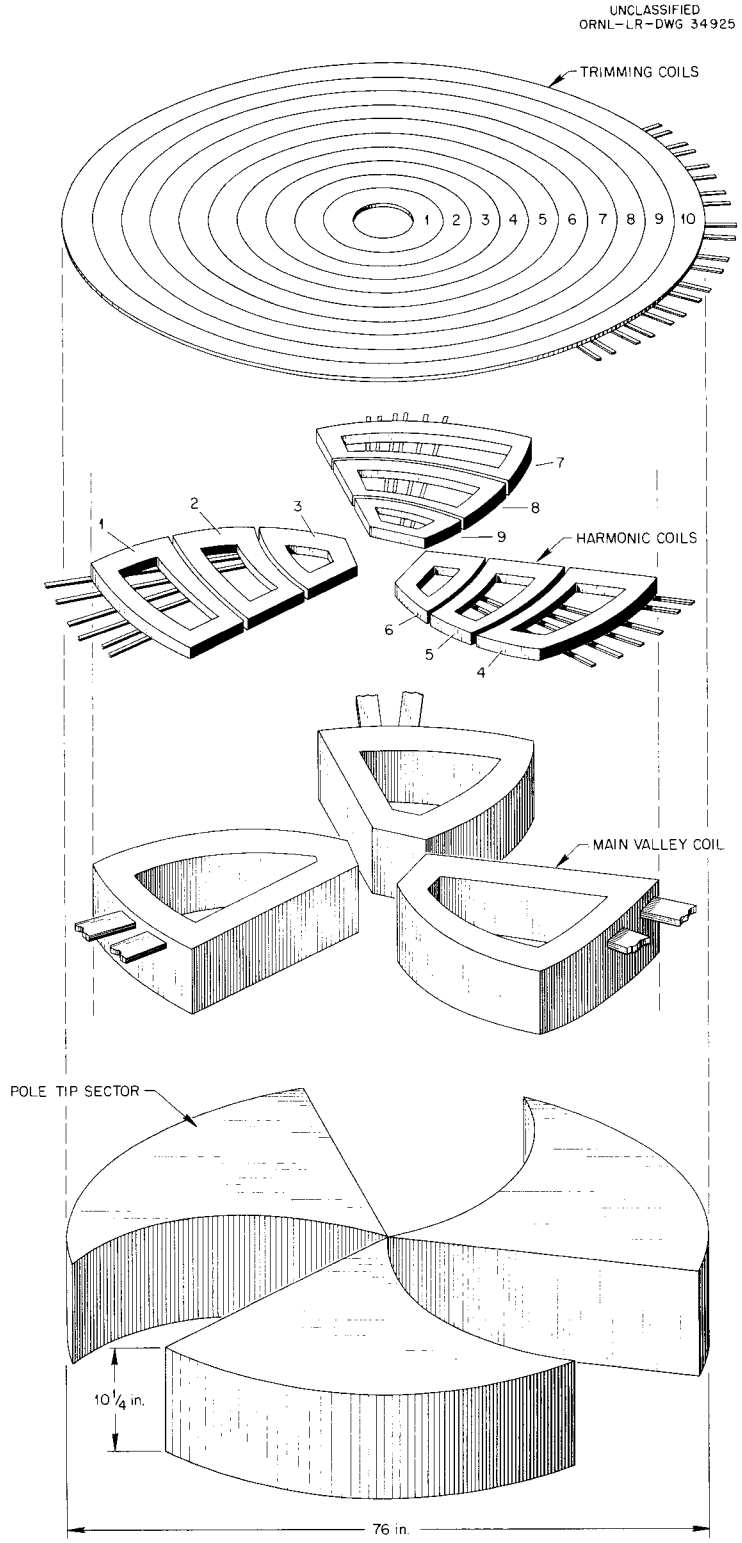

Fig. 23. Exploded View of a Pole Tip with Coils.

obtained in a model magnet of this configuration is shown in Fig. 24. The more important design characteristics may be summarized as follows:

Magnet Data	
Magnet field configuration	3-sector
Magnet core diameter	76 in.
Magnet pole tip diameter	76 in.
Beam radius, average maximum	31.5 in.
Magnet gap, hill	7.5 in.
valley	28.5 in.
Central magnetic field, maximum average	17 kilogauss
Magnet field rise with radius (max)	8%
Magnet excitation	1.23×10^6 amp-turns
Magnet weight	208 tons
Magnet cooling	Water
R-F System	
Dee diameter	71 in.
Dee aperture	1.87 in.
Dee-to-dee gap	2 in.
Oscillator tube	RCA 6949
Oscillator input power	650 kw max
Oscillator output power	500 kw max
Frequency	22.5 to 7.5 Mc/sec
As 3rd and 5th harmonics	7.5 to 1.5 Mc/sec
Bias	-1000 v
Miscellaneous	
Beam extraction type	Regenerative
Ion source	Hot cathode
Shielding	7 ft of ordinary concrete
Beam Power	
Protons	75 kw (1 ma protons at 75 Mev; other ions comparable)

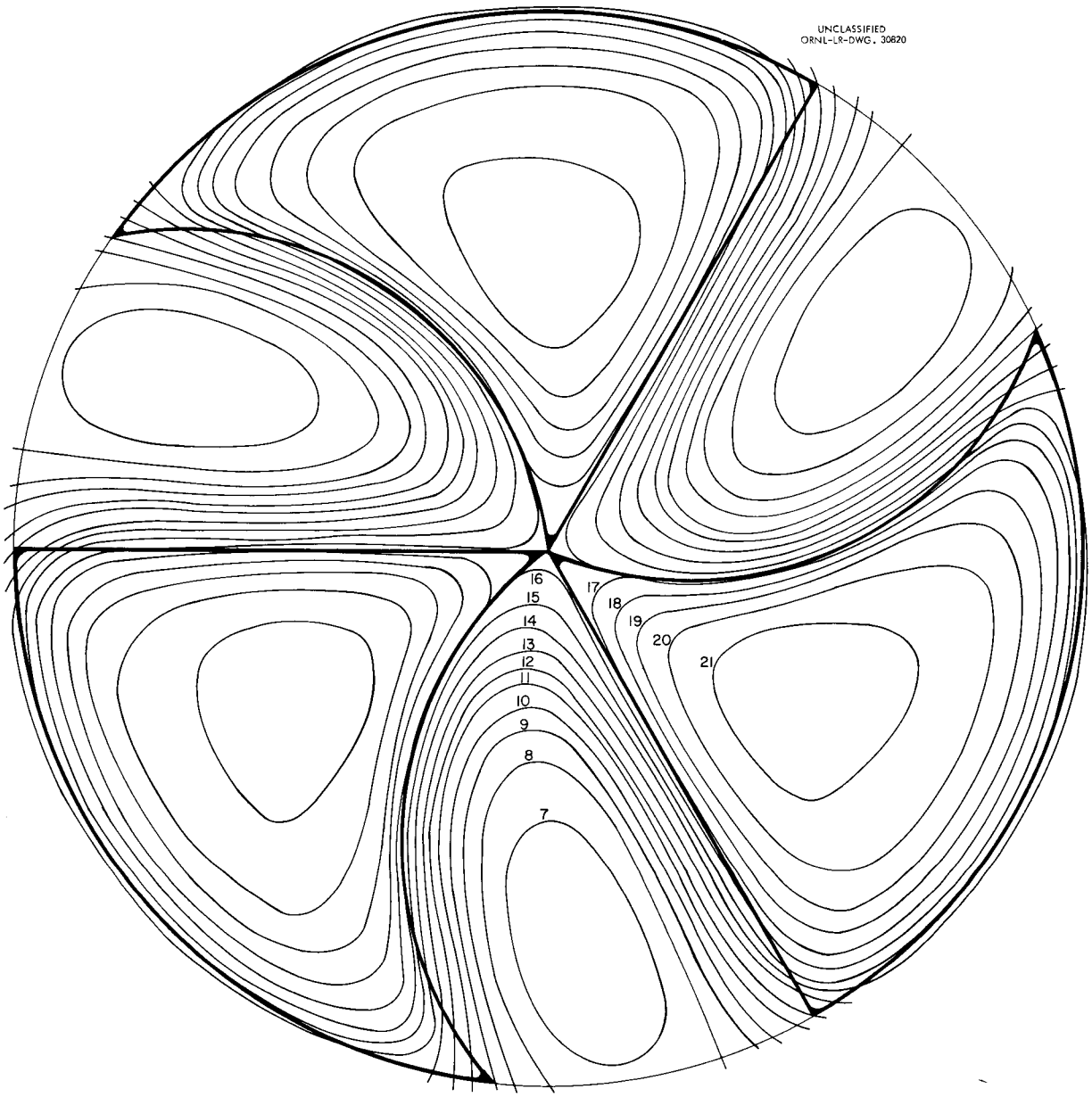

Fig. 24. Field Contours of the Three-Sector, Weak-Spiral Magnet, Sector Coils Energized (Magnetic Field in Kilogauss).

PUBLICATIONS

Previous Progress Reports

Progress reports have been issued by the Electronuclear Research Division for the periods ending on the dates listed below:

Y-495	September 30, 1949
Y-548	December 31, 1949
Y-584	March 31, 1950
Y-637	June 30, 1950
Y-676	September 30, 1950
Y-722	December 31, 1950
Y-767	March 31, 1951
Y-795	June 30, 1951
ORNL-1173	September 30, 1951, Part I
ORNL-1235	September 30, 1951, Part II
ORNL-1269	December 31, 1951, Part I
ORNL-1270	December 31, 1951, Part II
ORNL-1315	March 31, 1952, Part II
ORNL-1339	March 31, 1952, Part I
ORNL-1345	June 30, 1952, Part I
ORNL-1346	June 30, 1952, Part II
ORNL-1383	September 30, 1952
ORNL-1531	March 20, 1953
ORNL-1663	September 20, 1953
ORNL-1670	March 20, 1954
ORNL-1795	September 20, 1954
ORNL-1884	March 20, 1955
ORNL-2030	September 20, 1955
ORNL-2139	March 20, 1956
ORNL-2140	March 20, 1956
ORNL-2434	October 1, 1957

Papers Presented During the Period October 1, 1957–October 1, 1958

American Nuclear Society, New York City, October 1957.

E. E. Gross, "Two-Group Hand Calculations for the Army Package Power Reactor."

All-Union Conference on Nuclear Reactions at Low and Medium Energies, Moscow, USSR, November 1957.

B. L. Cohen, "Coincidence Studies of the $Ni^{58}(p,2p)$ Reaction."

B. L. Cohen, "Recent Studies of Anomalous Inelastic Proton Scattering."

American Physical Society, St. Louis, Missouri, November 1957.

T. J. Ward, J. W. Mihelich, B. Harmatz, and T. H. Handley, "Electron Capture of Hf^{173} to Levels in Lu^{173}."

American Physical Society, New York City, January 1958.

B. L. Cohen and A. G. Rubin, "Magnetic Analysis Studies of 23-Mev Proton Inelastic Scattering."

C. B. Fulmer and B. L. Cohen, "23-Mev Proton Induced (p,α) Reactions."

C. D. Goodman and K. S. Lee, "Level Density in Ne^{22}."

M. L. Halbert, J. J. Pinajian, and A. Zucker, "Nitrogen-Induced Nuclear Reactions in Potassium."

A. G. Rubin and B. L. Cohen, "Miscellaneous Investigations of Anomalous Inelastic Scattering."

A. Zucker, "Alpha Particles and Protons from the Nitrogen Bombardment of Aluminum."

Southeastern Section of the American Physical Society, Huntsville, Alabama, April 10–12, 1958.

B. L. Cohen, "Observations on Low and Medium Energy Physics in USSR."

C. B. Fulmer, "Fission Cross Section for 23-Mev Protons on U^{238}."

C. D. Goodman and A. Zucker, "Comparison of Level Densities for Nuclei of Different Even-Odd Character from Nitrogen-Induced Reactions."

R. S. Livingston, "Summary of Progress on the Southern Regional Accelerator."

J. A. Martin, R. S. Bender, and C. D. Goodman, "Experiments with a 4-Sector AVF Electron Cyclotron."

American Physical Society, Washington, D. C., May 1–3, 1958.

H. G. Blosser, E. D. Hudson, R. S. Lord, and B. D. Williams, "Magnet Design System for Azimuthally Varying Field (AVF) Cyclotron."

H. G. Blosser and F. Irwin, "Grid Focusing Studies in Cyclotron Central Region."

B. L. Cohen and A. G. Rubin, "23-Mev Proton Induced (p,p'), (p,d), and (p,t) Reactions."

D. E. Fisher, "Nuclear Reaction Cross Sections from the Nitrogen Bombardment of Sulfur."

Conference on Reactions Between Complex Nuclei, Gatlinburg, Tennessee, May 5–7, 1958.

C. D. Goodman, "Odd-Even Effects in Evaporation Reactions."

M. L. Halbert, "Elastic Scattering of N^{14} by Be^{9}."

J. J. Pinajian, "Nuclear Chemistry of the Low-Z Region."

A. Zucker, "Angular and Energy Distributions of Protons and Alpha Particles from N-O and N-Al Reactions."

International Congress of Nuclear Physics, Paris, France, July 7–11, 1958.

B. L. Cohen, "Direct Interactions – Experimental."

B. L. Cohen, A. G. Rubin, and C. B. Fulmer, "Nuclear Reaction Studies with 23-Mev Protons."

A. Zucker, "Nuclear Reactions and Scattering with 28-Mev N^{3+} Ions."

A. Zucker, "Nuclear Reactions Induced by Heavy Ions."

Articles Published During the Period October 1, 1957–October 1, 1958

H. G. Blosser, C. D. Goodman, and T. H. Handley, "Measurements of (n,α) Cross Sections at 14 Mev," Phys. Rev. 110, 531–533 (1958).

B. L. Cohen, "Coincidence Studies of the $Ni^{58}(p,2p)$ Reaction," Phys. Rev. 108, 768–773 (1957).

B. L. Cohen and C. B. Fulmer, "Fission-Fragment Mass Separator and the Nuclear Charge Distribution of Fission Fragments of a Single Mass," Nuclear Phys. 6, 547–560 (1958).

C. B. Fulmer, "Scintillation Response of CsI(Tl) Crystals to Fission Fragments and Energy vs Range in Various Materials for Light and Heavy Fission Fragments," Phys. Rev. 108, 1113–1116 (1957).

C. B. Fulmer and B. L. Cohen, "Equilibrium Charges of Fission Fragments in Gases," Phys. Rev. 109, 94 (1958).

C. B. Fulmer and B. L. Cohen, "Magnetic Analysis of the Long-Range Particles from Fission of U^{235}," Phys. Rev. 108, 370–372 (1957).

C. D. Goodman and J. L. Need, "Energy Distributions of Product Particles from Nitrogen-Induced Nuclear Reactions on Beryllium," Phys. Rev. 110, 676–682 (1958).

M. L. Halbert and A. Zucker, "Angular Distribution of N^{13} from N^{14} on Mg^{25}," Phys. Rev. 108, 336–341 (1957).

R. S. Livingston and J. A. Martin, "Electromagnetic Separation of the Isotopes of the Heavy Elements," Proceedings of the Symposium on Isotope Separation, Amsterdam VIII, 597–609 (1957).

R. S. Livingston and J. A. Martin, "Special Isotope Separator for Identification or Purification of Radioactive Species," Proceedings of the Symposium on Isotope Separation, Amsterdam VIII, 610–614 (1957).

J. W. Mihelich, B. Harmatz, and T. H. Handley, "Nuclear Spectroscopy of Neutron-Deficient Rare Earths (Tb Through Hf)," Phys. Rev. 108, 989–999 (1957).

A. Zucker, "Protons and Alpha-Particles from the Nitrogen Bombardment of Aluminum," Nuclear Phys. 6, 420–433 (1958).

Articles Submitted for Publication October 1, 1957–October 1, 1958

H. G. Blosser, R. E. Worsham, C. D. Goodman, R. S. Livingston, J. E. Mann, H. M. Moseley, G. T. Trammel, and T. A. Welton, "Four-Sector Azimuthally Varying Field Cyclotron," to Rev. Sci. Instr.

B. L. Cohen, "Cyclotrons and Synchrocyclotrons," for inclusion in Handbuch der Physik, Springer, Berlin.

B. L. Cohen and A. G. Rubin, "Improved Resolution and Other Recent Studies of Anomalous Inelastic Proton Scattering," to Phys. Rev.

B. L. Cohen and A. G. Rubin, "Inelastic Proton Scattering in Medium-Weight Elements," to Phys. Rev.

D. E. Fisher, A. Zucker, and A. Gropp, "Nuclear Reactions Induced by the Nitrogen Bombardment of Sulfur," to Phys. Rev.

C. B. Fulmer and B. L. Cohen, "23-Mev Proton-Induced (p,α) Reactions," to Phys. Rev.

F. L. Green and J. A. Martin, "Maximizing Production of Radioisotopes in a Cyclotron," to Nuclear Sci. and Eng.

F. L. Green and J. A. Martin, "The Use of Enriched Isotopes in the Cyclotron Production of Radioisotopes," to Nuclear Sci. and Eng.

J. J. Pinajian and M. L. Halbert, "Nitrogen-Induced Nuclear Reactions in Potassium," to Phys. Rev.

ANNOUNCEMENTS

R. S. Bender of University of Pittsburgh, C. E. Hunting of Massachusetts Institute of Technology, and S. W. Mosko of Drexel Institute of Technology have joined the Division. H. G. Blosser left for Michigan State University and A. G. Rubin for Williamson Development Co., M. H. Shelton has returned to graduate school, and B. L. Cohen is on leave to University of Pittsburgh.

The Electronuclear Research Division sponsored a conference[1] on reactions between complex nuclei at Gatlinburg, Tennessee, May 5–7, 1958. Twenty-five papers were presented to a total of over eighty participants, including guests from Canada, England, France, and Sweden.

(Added in proof) – Construction of the Oak Ridge Relativistic Isochronous Cyclotron has been approved. It will be installed in a new building east of Building 4500 at X-10 at a total estimated cost of $3,000,000.

---

[1]A. Zucker *et al.*, *Proceedings of the Conference on Reactions Between Complex Nuclei*, ORNL-2606 (May 1958).

ORNL-2740
Physics and Mathematics
(TID-4500 (14th ed.)

INTERNAL DISTRIBUTION

1. C. E. Center
2. Biology Library
3. Health Physics Library
4-6. Central Research Library
7. Reactor Experimental Engineering Library
8-11. Laboratory Records Department
12. Laboratory Records, ORNL R.C.
13. A. M. Weinberg
14. L. B. Emlet (K-25)
15. J. P. Murray (Y-12)
16. J. A. Swartout
17. E. H. Taylor
18. E. D. Shipley
19. S. C. Lind
20. M. L. Nelson
21. W. H. Jordan
22. R. R. Dickison
23. C. P. Keim
24. R. S. Livingston
25. F. L. Culler
26. H. G. Blosser
27. A. H. Snell
28. A. Hollaender
29. M. T. Kelley
30. G. E. Boyd
31. K. Z. Morgan
32. T. A. Lincoln
33. A. S. Householder
34. C. S. Harrill
35. C. E. Winters
36. H. E. Seagren
37. D. Phillips
38. P. M. Reyling
39. G. C. Williams
40. R. J. Jones
41. C. D. Goodman
42. F. T. Howard
43. R. E. Worsham
44. J. A. Martin
45. M. B. Marshall
46. A. Zucker
47. R. W. Johnson
48. J. A. Lane
49. M. J. Skinner
50. R. A. Charpie
51. R. F. Christy (consultant)
52. W. A. Fowler (consultant)
53. H. Feshback (consultant)
54. M. Goldhaber (consultant)
55. M. S. Livingston (consultant)
56. N. F. Ramsey (consultant)
57. J. R. Richardson (consultant)
58. J. H. Van Vleck (consultant)
59. J. A. Wheeler (consultant)
60. ORNL - Y-12 Technical Library, Document Reference Section

EXTERNAL DISTRIBUTION

61. Division of Research and Development, AEC, ORO
62-676. Given distribution as shown in TID-4500 (14th ed.) under Physics and Mathematics category (75 copies - OTS)